DIPARTIMENTO DI
ECONOMIA POLITICA
E STATISTICA
— DEPS

unisi

QUADERNI DEPS 951/2026

LUCKY LOSERS: FATIGUE, STRATEGIC REVERSALS, AND TERRITORIAL DYNAMICS

Andrea Caravaggio
Alessio Carrozzo Magli

November 2026



UNIVERSITÀ
DI SIENA
1240

Working Paper Series of the Department of Economics and Statistics of the University of Siena
Piazza San Francesco 7-8, 53100, Siena | Italy
deps.unisi.it

ISSN: 17209668

Lucky Losers: Fatigue, Strategic Reversals, and Territorial Dynamics

Andrea Caravaggio* Alessio Carrozzo Magli†

Abstract

Military superiority may not translate into long-run strategic advantage when sustained effort generates fatigue and recovery capacity differs across opponents. We develop a dynamic contest model in which military effort simultaneously increases the probability of success and contributes to the accumulation of fatigue, while replenishment allows fighting capacity to recover. The nonlinear fatigue dynamics generate multiple long-run regimes, endogenous recovery thresholds, and path dependence. We show that a player initially advantaged by lower vulnerability to fatigue may exert greater effort and become trapped in a high-fatigue regime, while a weaker opponent optimally restrains effort, recovers, and eventually reverses the balance of power. In a separable exponential contest, this reversal is established in a globally verified Markov-perfect equilibrium and can occur before recovery is complete. Extending the framework to state-dependent territorial competition, we characterize regime-dependent territorial reversals and switching cascades. We complement the theoretical analysis with historical evidence from militarized interstate disputes, using fertility differentials to instrument relative military manpower recovery. The instrumental-variable estimates reveal a positive and statistically significant relationship between relative recovery and dispute success. Together, the findings highlight how fatigue, replenishment, and initial conditions shape the evolution and long-run outcomes of military contests.

Keywords: dynamic contests; war fatigue; multiple steady states; state dependence; path dependence; regime switching.

JEL Classification: D74, C73, C61, F51.

*Department of Economics and Statistics (DEPS), University of Siena.
Email: andrea.caravaggio@unisi.it.

†University of Bologna. Email: alessio.carrozzo2@unibo.it.

1 Introduction

Military superiority is not necessarily durable. A state may enjoy an initial advantage in a confrontation and yet be less capable of sustaining military effort over time. Fighting depletes resources, imposes cumulative organizational and human costs, and changes the conditions under which subsequent effort is chosen. Conversely, a contestant that initially appears weaker may recover more effectively, rebuild its fighting capacity, and eventually overturn the balance of power. The outcome of a prolonged confrontation may therefore depend not only on how much military strength each side can deploy today, but also on how its ability and willingness to fight evolve tomorrow.

This distinction matters for the economic analysis of conflict. A large literature studies how contestants allocate resources to appropriation and defense and how these choices determine the distribution of contested resources (Hirshleifer, 1989; Garfinkel and Skaperdas, 2007). The bargaining literature, in turn, emphasizes private information, commitment problems, and changing incentives as conflict unfolds (Fearon, 1995; Powell, 2004). These approaches provide foundations for understanding the incentives to fight, but prolonged conflict also raises questions about how fighting changes the contestants' future capacity to compete.

Two complementary strands of the literature provide the main foundations for our analysis. The first investigates the intertemporal consequences of effort in dynamic contests. Keskin and Sağlam (2022) introduce accumulated fatigue and recovery into an infinite-horizon contest, characterizing open-loop stationary behavior and showing how differences in recovery rates shape competitive advantage. Angelova et al. (2022) further investigate the allocation of effort across fatigue-linked tournaments, identifying incentives for strategic resting and examining their behavioral relevance experimentally. These contributions establish that current competitive effort can impose a future burden, making restraint a potentially valuable strategic choice. A second strand focuses on the endogenous evolution of military strength through territorial outcomes. Beviá and Corchón (2013) show how the resources acquired in a contest may either reinforce or attenuate subsequent differences in competitive strength. More recently, Doğan et al. (2023) develop an infinite-horizon model of bargaining and war in which territorial holdings determine future military power, and characterize a unique Markov-perfect equilibrium encompassing different patterns of warfare, concessions, and border formation. While these models establish the importance of territorial feedbacks, the latter framework assigns a permanent attacking role to one state and does not incorporate the endogenous accumulation and recovery of military fatigue. Taken together, these two strands provide important insights into the intertemporal costs of fighting and the endogenous evolution of military strength, but leave less explored how the accumulation and recovery of fatigue may

themselves reshape the relative strategic position of competing states. In particular, while territorial gains can reinforce future military power, differences in the ability and incentives to sustain military effort may work in the opposite direction, potentially undermining an initial advantage. This raises a further question: can the recovery of one contestant not only reverse the prevailing balance of power, but also alter the opponent's subsequent prospects of recovery and the long-run distribution of territorial control?

We develop a continuous-time contest model in which two players choose costly military effort while accumulating fatigue. Current effort raises the probability of success but also adds to a fatigue stock that makes future fighting more costly. Fatigue is partially offset by a replenishment parameter, which can represent the replacement of personnel, organizational renewal, or other sources of restored fighting capacity. The law of motion is nonlinear, allowing persistent high-fatigue states to coexist with a low-fatigue recovery regime. This feature generates a threshold: depending on initial conditions and equilibrium effort, a player may recover or remain trapped in a persistently fatigued position. Importantly, the threshold is itself affected by strategic choices.

Our first result identifies a counterintuitive trade-off between immediate military effectiveness and dynamic resilience. A player that is less vulnerable to fatigue has a stronger incentive to exert effort and can enjoy a higher contemporaneous probability of success. But greater effort also reduces the set of fatigue states from which recovery is possible. By contrast, a more fatigue-vulnerable player restrains its effort, potentially preserving a path toward recovery. Thus, an initial advantage in fighting incentives need not translate into a lasting advantage in the contest. The mechanism does not rely on a reversal of primitive military capabilities: it arises because the two players' optimal responses to fatigue alter their subsequent capacity to compete.

We first establish this mechanism in a separable exponential contest. The specification delivers closed-form stationary efforts and a transparent characterization of the fatigue thresholds. More importantly, under explicit coexistence conditions, we verify a globally optimal Markov feedback policy. Along a recovery path, effort increases gradually as fatigue declines. Consequently, when one player remains in the high-fatigue regime while the other recovers, the ranking of success probabilities can reverse *before* the recovering player reaches the fatigue boundary. This result distinguishes the equilibrium transition from a mechanical comparison of stationary regimes: anticipation of recovery already affects optimal behavior along the path.

We then extend the environment to allow contest success to depend on previously controlled territory. Territory becomes a second state variable, and military effort affects both the immediate probability of success and the subsequent distribution of control. The model

admits distinct stationary configurations in which neither player, one player, or both players have fully recovered. A switch in fatigue status changes the stationary territorial target and can therefore reverse the identity of the long-run majority controller. It can also alter the opponent's regime-specific stationary effort and associated fatigue threshold, creating the possibility of switching cascades or of one player's recovery trapping the other in persistent fatigue under piecewise-stationary adjustment. These results characterize stationary regimes and transitions under an explicitly piecewise-stationary adjustment rule; unlike the separable case, they are not presented as a globally verified nonstationary Markov-perfect equilibrium. Numerical illustrations show how the order and timing of recovery can shape the eventual territorial allocation.

To investigate the empirical relevance of the recovery mechanism, we combine dyadic militarized interstate disputes with historical military-personnel and fertility data. We measure relative military recovery by whether state A's change in military personnel exceeds that of state B, instrumenting this measure with fertility differentials 15–18 years before the dispute. The underlying rationale is that past demographic conditions shape the availability of military-age cohorts and, consequently, states' capacity to replenish their armed forces. The results reveal a positive and statistically significant relationship between relative military recovery and dispute success, with IV estimates substantially larger than their OLS counterparts. This pattern suggests that demographically driven differences in military recovery may play an important role in shaping conflict outcomes, consistent with the model's central mechanism. While a causal interpretation remains conditional on the validity of the exclusion restriction, the empirical findings provide complementary support for the theoretical predictions.

Our contribution is to connect three elements that are often considered separately: the current return to military effort, the endogenous evolution of fighting capacity, and the possibility of changes in the ranking of contestants over time. The nonlinear fatigue law generates path dependence; optimal effort makes recovery thresholds strategic; and territorial state dependence transmits changes in fatigue regimes into persistent changes in control. In this sense, military strength is not simply a stock that determines the course of conflict. It is partly an outcome of the conflict process itself.

The remainder of the paper is organized as follows. Section 2 introduces the dynamic environment, the fatigue law, and the equilibrium concepts. Section 3 analyzes the state-independent exponential contest, characterizes its fatigue regimes, and establishes the optimal-feedback reversal result. Section 4 introduces territorial state dependence and studies stationary territorial outcomes, regime switching, and cascades. Section 5 illustrates the mechanisms numerically. Section 6 presents the empirical analysis of historical fertility, relative military-personnel changes, and dispute outcomes.

2 Dynamic contest framework and fatigue regimes

We consider two players, i and j, competing in continuous time for a prize of value $\pi > 0$. At each instant, player i chooses nonnegative military effort $g_i(t) \geq 0$ and carries a nonnegative stock of fatigue $c_i(t) \geq 0$. Both players discount future payoffs at rate $r > 0$. Player i maximizes

$$J_i = \int_0^\infty \mathrm{e}^{-rt} \left[\pi p_i(t) - g_i(t) - \rho_i c_i(t)^2\right] \mathrm{d}t, \tag{2.1}$$

where $p_i(t)$ denotes the instantaneous probability of success and $\rho_i > 0$ measures vulnerability to fatigue. A larger ρ_i increases the cost associated with a given fatigue stock. The corresponding objective applies to player j.

Military effort increases current contest success but also contributes to the accumulation of fatigue. In the interior of the state space, fatigue evolves according to

$$\dot{c}_i(t) = g_i(t) + c_i(t) - c_i(t)^2 - k, \tag{2.2}$$

where k captures replenishment, replacement, or organizational renewal. The nonlinear term $c_i - c_i^2$ combines persistence in fatigue accumulation with a dampening effect at higher fatigue levels. As shown below, this reduced-form specification allows recovery to coexist with persistent high fatigue, generating threshold effects and path dependence.

We consider two specifications of the contest success function. The first is a separable exponential technology,

$$p_i(g_i, g_j) = \frac{1 + \mathrm{e}^{-g_j} - \mathrm{e}^{-g_i}}{2}, \tag{2.3}$$

with $p_j = 1 - p_i$. Its separability makes the players' optimal-effort problems tractable and allows a global verification of equilibrium strategies under the conditions specified in Section 3.

The second specification introduces dependence on previously controlled territory:

$$p_i(g_i, g_j, x_i) = \frac{1 + x_i \mathrm{e}^{-g_j} - (1 - x_i)\mathrm{e}^{-g_i}}{2}, \tag{2.4}$$

where $x_i(t) \in [0, 1]$ denotes the territorial share controlled by player i. Territory evolves according to

$$\dot{x}_i(t) = p_i(g_i, g_j, x_i) - x_i(t). \tag{2.5}$$

Thus, current contest success affects future territorial control, which in turn influences the marginal effectiveness of military effort.

Throughout the closed-form analysis, we impose

$$r = 1. \tag{2.6}$$

This restriction simplifies the stationary costate equations, but is substantive relative to the unit coefficient on c_i in the fatigue dynamics. In particular, the global dynamic verification developed in Section 3 applies under this restriction.

Since fatigue cannot be negative, its evolution is governed by the projected state law

$$\dot{c}_i = \begin{cases} g_i + c_i - c_i^2 - k, & c_i > 0, \\ \max\{g_i - k, 0\}, & c_i = 0. \end{cases} \tag{2.7}$$

The projection prevents negative fatigue stocks and allows a player to sustain positive military effort at zero fatigue, provided that replenishment is sufficient.

We distinguish two fatigue regimes, according to whether the fatigue stock is positive or has reached its lower boundary.

Definition 1 (Fatigue regimes)**.** *Player i is in an interior fatigue regime, denoted by* I*, when its stationary fatigue stock satisfies $c_i > 0$. It is in a boundary fatigue regime, denoted by* B*, when $c_i = 0$. A regime profile is an element*

$$R = (R_i, R_j) \in \{\mathrm{I}, \mathrm{B}\}^2.$$

At an interior stationary point, the current-value costate associated with fatigue satisfies

$$\lambda_i^{\mathrm{I}} = -\rho_i. \tag{2.8}$$

At the boundary, we adopt the stationary zero-shadow-value selection

$$\lambda_i^{\mathrm{B}} = 0. \tag{2.9}$$

For the separable contest, this boundary value is established by the Hamilton–Jacobi–Bellman verification in Section 3 under the relevant parameter restrictions. In the state-dependent contest, it remains an adopted selection rather than a globally verified boundary condition.

We summarize the regime-dependent marginal effort wedge as

$$a_i^R := 1 - \lambda_i^R = \begin{cases} 1 + \rho_i, & R_i = \mathrm{I}, \\ 1, & R_i = \mathrm{B}. \end{cases} \tag{2.10}$$

This notation records whether the fatigue shadow cost is active without introducing additional primitive parameters.

Assumption 1 (Interior effort)**.** *Whenever an interior first-order condition is used, parameters satisfy the corresponding strict positivity condition for effort. Corner solutions at $g_i = 0$ are economically relevant but are not the focus of the closed-form regime analysis.*

The two contest technologies require distinct solution concepts. For the separable exponential contest, Section 3 characterizes stationary regimes and globally verifies a Markov-perfect equilibrium in feedback strategies under explicit parameter restrictions. During optimal recovery, effort generally varies with the fatigue stock.

For the state-dependent contest, Section 4 characterizes candidate stationary configurations using the regime-specific stationarity conditions and the adopted boundary-costate selection. To study transitions, we employ a piecewise-stationary adjustment rule: efforts are held at their regime-specific stationary values and updated when a fatigue stock reaches zero. The resulting trajectories are exact conditional on this rule, but are not claimed to constitute nonstationary Nash equilibrium paths.

3 Separable exponential success without state dependence

The state-independent exponential success function is

$$p_i(g_i, g_j) = \frac{1 + \mathrm{e}^{-g_j} - \mathrm{e}^{-g_i}}{2}, \qquad p_j = 1 - p_i. \tag{3.1}$$

Its main tractability property is separability:

$$\frac{\partial p_i}{\partial g_i} = \frac{\mathrm{e}^{-g_i}}{2}.$$

The marginal return to player i's effort does not depend on g_j. Strategic interaction remains in success probabilities and payoffs, but stationary effort choices are individually separable.

3.1 Stationary effort, success, and the static benchmark

Proposition 1 (Closed-form stationary effort and success)**.** *Consider a regime profile* $R \in \{\mathrm{I}, \mathrm{B}\}^2$*. Under Assumption 1, stationary effort is*

$$g_i^R = \ln\left(\frac{\pi}{2a_i^R}\right), \qquad g_j^R = \ln\left(\frac{\pi}{2a_j^R}\right). \tag{3.2}$$

The associated success probabilities are

$$p_i^R = \frac{1}{2} + \frac{a_j^R - a_i^R}{\pi}, \qquad p_j^R = 1 - p_i^R. \tag{3.3}$$

In particular,

$$p_i^{\mathrm{II}} = \frac{1}{2} + \frac{\rho_j - \rho_i}{\pi}, \tag{3.4}$$

$$p_i^{\mathrm{BI}} = \frac{1}{2} + \frac{\rho_j}{\pi}, \tag{3.5}$$

$$p_i^{\mathrm{IB}} = \frac{1}{2} - \frac{\rho_i}{\pi}, \tag{3.6}$$

$$p_i^{\mathrm{BB}} = \frac{1}{2}. \tag{3.7}$$

The boundary effort

$$g_i^{\mathrm{B}} = \ln\left(\frac{\pi}{2}\right) \tag{3.8}$$

coincides with the static exponential-contest solution. The interior fatigue regime reduces effort by

$$g_i^{\mathrm{B}} - g_i^{\mathrm{I}} = \ln(1 + \rho_i) > 0. \tag{3.9}$$

Thus fatigue acts as an endogenous marginal wedge rather than merely an additive payoff loss.

Remark 1 (Admissibility)**.** *Positive interior effort requires*

$$\pi > 2a_i^R.$$

For an interior fatigue player this is $\pi > 2(1 + \rho_i)$*; for a boundary player it is* $\pi > 2$*. These restrictions also ensure that the probabilities displayed above remain in the unit interval in the mixed regimes considered below.*

3.2 Fatigue phase portrait and exact transition paths

Fix a constant regime effort $g \geq 0$. The interior fatigue equation is

$$\dot{c} = g + c - c^2 - k. \tag{3.10}$$

Define

$$\Delta(g) := 1 + 4(g - k). \tag{3.11}$$

When $\Delta(g) \geq 0$, define

$$c^-(g) = \frac{1 - \sqrt{\Delta(g)}}{2}, \qquad c^+(g) = \frac{1 + \sqrt{\Delta(g)}}{2}. \tag{3.12}$$

Proposition 2 (Complete classification of fatigue dynamics)**.** *Under the projected state law* (2.7)*, the fatigue dynamics conditional on constant effort g satisfy the following classification.*

(i) If $k < g$, the lower root is negative, the boundary is not viable, and every $c(0) \geq 0$ converges to the unique positive stable state $c^+(g) > 1$.

(ii) If $k = g$, the stationary states are 0 and 1. The boundary is stationary only when reached exactly and is unstable from the right; every $c(0) > 0$ converges to 1.

(iii) If

$$g < k < g + \frac{1}{4}, \tag{3.13}$$

then

$$0 < c^-(g) < \frac{1}{2} < c^+(g) < 1.$$

The boundary $c = 0$ and the high-fatigue state $c^+(g)$ are stable under the projected state dynamics, while $c^-(g)$ is an unstable threshold:

$$0 \leq c(0) < c^-(g) \Longrightarrow c(t) \to 0, \tag{3.14}$$

$$c(0) > c^-(g) \Longrightarrow c(t) \to c^+(g). \tag{3.15}$$

(iv) If $k = g + \frac{1}{4}$, the two interior roots coalesce at $c = 1/2$. The point $1/2$ is semistable, while initial conditions below it reach the boundary.

(v) If $k > g + \frac{1}{4}$, no interior stationary fatigue stock exists and the boundary is globally attracting.

When $\Delta(g) > 0$, the unconstrained transition path is available in closed form. Let

$$R_0 = \frac{c(0) - c^-(g)}{c^+(g) - c(0)}.$$

Then, until the boundary is reached,

$$c(t) = \frac{c^-(g) + c^+(g) R_0 \mathrm{e}^{\sqrt{\Delta(g)}t}}{1 + R_0 \mathrm{e}^{\sqrt{\Delta(g)}t}}. \tag{3.16}$$

If $0 < c(0) < c^-(g)$, the hitting time of the boundary is

$$T_0 = \frac{1}{\sqrt{\Delta(g)}} \ln \left[\frac{c^-(g)\big(c^+(g) - c(0)\big)}{c^+(g)\big(c^-(g) - c(0)\big)} \right]. \tag{3.17}$$

The economically central region is (3.13). A player below $c^-(g)$ recovers fully, whereas a player above it remains permanently fatigued. The unstable threshold is therefore a measure of the size of the recovery region.

In the parameter region imposed below, this same threshold turns out to be the *optimal-policy* separatrix, not merely the separatrix generated by the constant control g^{I}. This stronger conclusion requires a value function and an HJB verification; it cannot be inferred from the phase portrait alone.

Proposition 3 (Canonical stability qualification)**.** *For the unconstrained state-independent optimal-control subsystem, the interior stationary points are*

$$\big(c^-(g_i^{\mathrm{I}}), -\rho_i\big) \quad \textit{and} \quad \big(c^+(g_i^{\mathrm{I}}), -\rho_i\big).$$

The lower stationary point is a source in the canonical (c_i, λ_i) system. The high-fatigue stationary point is a saddle. Its eigenvalues are

$$1 - 2c_i^+ < 0 \qquad \textit{and} \qquad 2c_i^+ > 0. \tag{3.18}$$

Proposition 3 clarifies the interpretation of the basin analysis. The threshold c^- is an unstable threshold of the reduced state law conditional on a stationary regime. In the full open-loop problem, the costate is forward-looking and the economically relevant high-fatigue steady state is saddle-point stable.

3.3 Coexistence of fatigue regimes

A boundary regime must be viable under its own boundary effort. An interior high-fatigue regime must possess a real positive high root under its own interior effort.

Proposition 4 (Coexistence of boundary and high-fatigue regimes)**.** *For player i, a persistent boundary regime and an interior high-fatigue regime can coexist if and only if*

$$g_i^{\mathrm{B}} \leq k < g_i^{\mathrm{I}} + \frac{1}{4}. \tag{3.19}$$

The coexistence interval is nonempty if and only if

$$\ln(1+\rho_i) < \frac{1}{4}. \tag{3.20}$$

If

$$g^{\mathrm{B}} \leq k < \min\left\{ g_i^{\mathrm{I}} + \frac{1}{4},\, g_j^{\mathrm{I}} + \frac{1}{4} \right\}, \tag{3.21}$$

then all four regime profiles

$$(\mathrm{I},\mathrm{I}), \quad (\mathrm{B},\mathrm{I}), \quad (\mathrm{I},\mathrm{B}), \quad (\mathrm{B},\mathrm{B})$$

are stationary-regime consistent.

Condition (3.19) contains two forces. The lower inequality ensures that the high effort selected at the boundary does not regenerate fatigue. The upper inequality ensures that the interior high-fatigue state has not disappeared. Coexistence is therefore possible only when the effort increase caused by eliminating the fatigue shadow cost is not too large.

3.4 Comparative statics of the recovery region

Proposition 5 (Weakness as a commitment to restraint)**.** *In the interior exponential regime,*

$$\frac{\partial g_i^{\mathrm{I}}}{\partial \rho_i} = -\frac{1}{1+\rho_i} < 0. \tag{3.22}$$

Within the bistability region,

$$\frac{\partial c_i^{-}(g_i^{\mathrm{I}})}{\partial \rho_i} = \frac{1}{(1+\rho_i)\sqrt{1+4(g_i^{\mathrm{I}}-k)}} > 0, \tag{3.23}$$

$$\frac{\partial c_i^{+}(g_i^{\mathrm{I}})}{\partial \rho_i} = -\frac{1}{(1+\rho_i)\sqrt{1+4(g_i^{\mathrm{I}}-k)}} < 0. \tag{3.24}$$

A more fatigue-vulnerable player exerts less effort, has a larger recovery region, and has a lower high-fatigue steady state.

This result produces a nonstandard form of resilience. A large ρ_i is a direct disadvantage because fatigue is more costly. Yet it also commits the player to restraint. Lower effort raises the unstable threshold, making it easier to remain in the low-fatigue basin. A player that is statically weaker may therefore be dynamically more likely to recover.

The comparative statics of $c^-(g^{\mathrm{I}})$ acquire a strategic interpretation once Proposition 6 is established: in its strict coexistence region, $c^-(g^{\mathrm{I}})$ is also the boundary between recovery under the *optimal* feedback and the high-fatigue optimal path.

3.5 Verified optimal feedback and pre-boundary strategic reversal

The separable exponential technology permits a complete dynamic Nash verification, not merely a comparison of stationary-regime candidates. Let $q := \pi/2$ and separate player i's payoff into a term independent of g_i and the one-player problem

$$\max_{g_i(\cdot)\geq 0} V_i(c_{i,0}) := \int_0^\infty \mathrm{e}^{-t}\big[f(g_i(t)) - \rho_i c_i(t)^2\big]\,\mathrm{d}t, \qquad f(g) = q(1-\mathrm{e}^{-g}) - g. \tag{3.25}$$

The omitted additive term is $\int_0^\infty \mathrm{e}^{-t} q \mathrm{e}^{-g_j(t)}\,\mathrm{d}t$; it does not change player i's best response. We work with measurable, nonnegative controls with finite discounted effort and fatigue costs, so that the standard terminal transversality term vanishes.

Assumption 2 (Strict recovery–high-fatigue coexistence)**.** *For each player under consideration,*

$$q > 1+\rho_i, \qquad g^{\mathrm{B}} := \ln q < k < g_i^{\mathrm{I}} + \frac{1}{4}, \qquad g_i^{\mathrm{I}} := \ln\frac{q}{1+\rho_i}. \tag{3.26}$$

Thus $0 < c_i^- := c^-(g_i^{\mathrm{I}}) < 1/2 < c_i^+ := c^+(g_i^{\mathrm{I}})$, $g_i^{\mathrm{I}} > 0$, *and the boundary is strictly inward pointing under* g^{B}.

In an interior fatigue state, the discounted HJB equation for (3.25) is

$$V_i(c) = \max_{g\geq 0}\big\{f(g) - \rho_i c^2 + V_i'(c)(g + c - c^2 - k)\big\}, \quad c > 0. \tag{3.27}$$

At $c = 0$ the projected drift is $\max\{g-k, 0\}$. For an interior optimal effort, the HJB first-order condition yields

$$g_i^*(c) = \ln\frac{q}{1 - V_i'(c)}. \tag{3.28}$$

To construct the recovery branch, solve the *backward* characteristic, parameterized by the time s remaining until fatigue reaches zero:

$$\frac{\mathrm{d}C_i}{\mathrm{d}s} = k - G_i(\Lambda_i) - C_i + C_i^2, \qquad C_i(0) = 0, \tag{3.29}$$

$$\frac{\mathrm{d}\Lambda_i}{\mathrm{d}s} = -2C_i(\Lambda_i + \rho_i), \qquad \Lambda_i(0) = 0, \tag{3.30}$$

where $G_i(\lambda) := \ln[q/(1-\lambda)]$. The characteristic satisfies $C_i'(s) > 0$, $C_i(s) \uparrow c_i^-$, and $\Lambda_i(s) \downarrow -\rho_i$ as $s \to \infty$. It therefore defines a single-valued function $\ell_i(c) := \Lambda_i(C_i^{-1}(c))$ on $[0, c_i^-)$, continuously extended by $\ell_i(c_i^-) = -\rho_i$. Here ℓ_i denotes the value-function slope and must *not* be confused with the regulator of the projected state constraint.

Define the constants

$$B := f(g^{\mathrm{B}}) = q - 1 - \ln q, \tag{3.31}$$

$$A_i := f(g_i^{\mathrm{I}}) - \rho_i g_i^{\mathrm{I}} + \rho_i k. \tag{3.32}$$

Proposition 6 (Global HJB verification and optimal recovery feedback)**.** *Under Assumption 2, the one-player value function is continuously differentiable and satisfies*

$$V_i(c) = \begin{cases} B + \displaystyle\int_0^c \ell_i(u)\,\mathrm{d}u, & 0 \le c \le c_i^-, \\ A_i - \rho_i c, & c \ge c_i^-. \end{cases} \tag{3.33}$$

A globally optimal stationary Markov policy is

$$g_i^*(c) = \begin{cases} \ln \dfrac{q}{1-\ell_i(c)}, & 0 < c < c_i^-, \\ g^{\mathrm{B}}, & c = 0, \\ g_i^{\mathrm{I}}, & c \ge c_i^-. \end{cases} \tag{3.34}$$

On the recovery interval $g_i^*(c)$ is strictly decreasing in c and satisfies $g_i^{\mathrm{I}} < g_i^*(c) < g^{\mathrm{B}}$. When $0 < c_i(0) < c_i^-$, fatigue decreases strictly, reaches zero in finite time, and $g_i^*(c_i(t))$ increases continuously *toward g^{B}. When $c_i(0) > c_i^-$, the optimal control is g_i^{I} and fatigue converges to c_i^+. The profile $(g_i^*(c_i), g_j^*(c_j))$ is a stationary Markov-perfect equilibrium of the separable contest and induces an open-loop Nash equilibrium from any given initial stocks.*

A complete proof of Proposition 6, including the global HJB verification and the transversality argument, is provided in Subsection A.4 of the Appendix.

The hitting time of the optimal recovery path differs from the constant-effort expression

(3.17). Instead it is

$$T_i(c_{i,0}) = \int_0^{c_{i,0}} \frac{\mathrm{d}c}{k - g_i^*(c) - c + c^2}, \qquad 0 < c_{i,0} < c_i^-. \tag{3.35}$$

The denominator is strictly positive on the recovery interval. The stationary interior formula g_i^{I} and the boundary value g^{B} are therefore only the endpoint values of an entire optimal feedback schedule, rather than two controls between which players optimally jump.

Proposition 7 (Equilibrium reversal *before* full recovery)**.** *Suppose both players satisfy Assumption 2 and $0 < \rho_i < \rho_j$. Let $c_{j,\times}$ be the unique point in $(0, c_j^-)$ satisfying*

$$\ell_j(c_{j,\times}) = -\rho_i \quad \Longleftrightarrow \quad g_j^*(c_{j,\times}) = g_i^{\mathrm{I}}. \tag{3.36}$$

If

$$c_i(0) > c_i^-, \qquad c_{j,\times} < c_j(0) < c_j^-, \tag{3.37}$$

then along the Markov-perfect equilibrium path player i exerts g_i^{I} for all time, while player j recovers and gradually increases effort. There is a unique time $t_\times$ strictly before j's boundary hitting time T_j at which

$$p_i(t) > \frac{1}{2}\ (t < t_\times), \qquad p_i(t_\times) = \frac{1}{2}, \qquad p_i(t) < \frac{1}{2}\ (t > t_\times). \tag{3.38}$$

In particular,

$$t_\times = \int_{c_{j,\times}}^{c_j(0)} \frac{\mathrm{d}c}{k - g_j^*(c) - c + c^2} \ < \ T_j(c_j(0)), \tag{3.39}$$

and the limiting success probability is

$$\lim_{t\to\infty} p_i(t) = \frac{1}{2} - \frac{\rho_i}{\pi} < \frac{1}{2}. \tag{3.40}$$

The parameter restrictions and the initial inequalities define a nonempty open region for such a pre-boundary reversal.

Corollary 1 (Stationary *flow* payoff comparison)**.** *At the long-run regime* (I, B)*, in which player i converges to c_i^+ and player j has $c_j = 0$, the stationary flow payoff difference is*

$$W_j^{\mathrm{IB}} - W_i^{\mathrm{IB}} = 2\rho_i - \ln(1 + \rho_i) + \rho_i (c_i^+)^2 > 0. \tag{3.41}$$

This does not *imply that player j necessarily receives the larger discounted payoff from arbitrary initial states.*

This result is sharper than a reversal caused by an instantaneous regime switch. In equilibrium, the opponent anticipates the diminishing future fatigue burden and begins raising effort *before* reaching $c_j = 0$. In particular, the success probability can cross one half while both fatigue stocks are still strictly positive. This conclusion is exact for the state-independent separable contest under Assumption 2; it does not establish analogous optimality for the state-dependent contest studied in Section 4.

3.6 Switching, shocks, and hysteresis

The state-independent model separates regime selection from strategic interaction. Conditional on a regime, effort is constant and fatigue follows an autonomous one-dimensional equation. Therefore, absent a change in parameters, policy, or the state constraint, a trajectory does not spontaneously move from the high-fatigue basin to the low-fatigue basin. A switch requires one of three events:

(a) an initial condition below the unstable threshold;

(b) a temporary change in k, π, or ρ_i that moves the threshold or the fatigue stock;

(c) a direct recovery shock that moves c_i below c_i^-.

A downward recovery shock $S_i > 0$ at time τ changes fatigue according to

$$c_i(\tau^+) = \max\{0, c_i(\tau^-) - S_i\}.$$

The minimum shock that moves the player into the recovery region is

$$S_i > c_i(\tau^-) - c_i^-(g_i^{\mathrm{I}}). \tag{3.42}$$

If the boundary remains viable after the original parameters are restored, the switch is persistent. This creates hysteresis: a temporary intervention can have a permanent effect because it changes the basin in which the state is located.

4 The state-dependent exponential contest

We now adopt the state-dependent specification

$$p_i(g_i, g_j, x_i) = \frac{1 + x_i \mathrm{e}^{-g_j} - (1 - x_i)\mathrm{e}^{-g_i}}{2}, \tag{4.1}$$

together with

$$\dot{x}_i = p_i(g_i, g_j, x_i) - x_i. \tag{4.2}$$

The interpretation differs from a technology in which territory enters the exponent. Here, $1 - x_i$ is the remaining territory that player i can gain, while x_i is the territory that player j can take back. Consequently,

$$\frac{\partial p_i}{\partial g_i} = \frac{(1 - x_i)\mathrm{e}^{-g_i}}{2}, \qquad \frac{\partial p_i}{\partial g_j} = -\frac{x_i \mathrm{e}^{-g_j}}{2}. \tag{4.3}$$

The territory state introduces a second shadow value. Nevertheless, all stationary regime profiles remain tractable.

4.1 Closed-form stationary regimes

For a regime profile R, retain the wedges a_i^R and a_j^R from (2.10). Define

$$y_i^R := \frac{\mathrm{e}^{-g_i^R}}{2}, \qquad y_j^R := \frac{\mathrm{e}^{-g_j^R}}{2}. \tag{4.4}$$

For notational economy, write $x = x_i$ and define

$$D_R(x) := 2\pi x(1 - x) + (1 - x)a_j^R + x a_i^R. \tag{4.5}$$

Proposition 8 (Stationary state-dependent equilibrium in any fatigue regime)**.** *Fix a regime profile $R \in \{\mathrm{I}, \mathrm{B}\}^2$. Under Assumption 1, a stationary equilibrium satisfies*

$$y_i^R(x) = \frac{2x a_i^R}{D_R(x)}, \tag{4.6}$$

$$y_j^R(x) = \frac{2(1 - x)a_j^R}{D_R(x)}, \tag{4.7}$$

$$g_i^R(x) = -\ln\left[\frac{4x a_i^R}{D_R(x)}\right], \tag{4.8}$$

$$g_j^R(x) = -\ln\left[\frac{4(1 - x)a_j^R}{D_R(x)}\right]. \tag{4.9}$$

The stationary territorial share $x_R^* \in (0, 1)$ solves

$$\begin{aligned} F_R(x) := {} & 4\pi x^3 - 2\left[3\pi + a_j^R - a_i^R\right] x^2 \\ & + \left[2\pi + a_j^R - 3a_i^R\right] x + a_j^R = 0. \end{aligned} \tag{4.10}$$

Once x_R^* is selected, stationary effort is obtained from (4.8)–(4.9)*, and*

$$p_i^R = x_R^*. \tag{4.11}$$

For the interior–interior regime, $a_i^{\mathrm{II}} = 1 + \rho_i$ and $a_j^{\mathrm{II}} = 1 + \rho_j$. Equation (4.10) becomes

$$4\pi x^3 - 2\left[3\pi + \rho_j - \rho_i\right] x^2 + \left[2\pi + \rho_j - 3\rho_i - 2\right] x + (1 + \rho_j) = 0, \tag{4.12}$$

which is the cubic obtained in the underlying calculations. Its Cardano representation is reported in Appendix B.

Remark 2 (Effort admissibility)**.** *The interior-effort restrictions are*

$$D_R(x_R^*) > 4x_R^* a_i^R, \qquad D_R(x_R^*) > 4(1 - x_R^*)a_j^R. \tag{4.13}$$

If either inequality fails, the corresponding effort is at the corner $g = 0$, and the relevant stationary system changes.

4.2 Uniqueness and territorial ordering

Although (4.10) has three algebraic roots over the complex numbers, the economically relevant stationary territorial share is unique.

Proposition 9 (Unique economic territorial root)**.** *For every $\pi > 0$ and $a_i^R, a_j^R > 0$, equation* (4.10) *has a unique root $x_R^* \in (0, 1)$. This root satisfies*

$$x_R^* \begin{cases} > \frac{1}{2}, & a_j^R > a_i^R, \\ = \frac{1}{2}, & a_j^R = a_i^R, \\ < \frac{1}{2}, & a_j^R < a_i^R. \end{cases} \tag{4.14}$$

The wedge a_i^R summarizes the effective marginal burden of effort. A lower own wedge relative to the opponent shifts the stationary territorial share in the player's favor. The result

immediately ranks the four regime profiles:

$$x^*_{\mathrm{BI}} > \frac{1}{2}, \tag{4.15}$$

$$x^*_{\mathrm{IB}} < \frac{1}{2}, \tag{4.16}$$

$$x^*_{\mathrm{BB}} = \frac{1}{2}, \tag{4.17}$$

$$x^*_{\mathrm{II}} > \frac{1}{2} \quad \Longleftrightarrow \quad \rho_i < \rho_j. \tag{4.18}$$

State dependence therefore preserves the basic advantage of reaching the boundary, but gives the advantage a territorial interpretation. The boundary player does not merely obtain a higher instantaneous probability; it becomes the unique long-run majority controller.

4.3 Territorial adjustment within a regime

Given constant regime efforts g_i^R, g_j^R, the territorial law is linear:

$$\dot{x}_i = \frac{1 - \mathrm{e}^{-g_i^R}}{2} - \left[1 - \frac{\mathrm{e}^{-g_i^R} + \mathrm{e}^{-g_j^R}}{2}\right] x_i. \tag{4.19}$$

Proposition 10 (Closed-form territorial transition)**.** *Let*

$$\gamma_R := 1 - y_i^R - y_j^R > 0. \tag{4.20}$$

Within a fixed regime profile R, territory follows

$$x_i(t) = x_R^* + [x_i(\tau) - x_R^*]\, \mathrm{e}^{-\gamma_R (t-\tau)}, \qquad t \geq \tau, \tag{4.21}$$

where

$$x_R^* = \frac{1 - 2y_i^R}{2(1 - y_i^R - y_j^R)}. \tag{4.22}$$

Thus the territorial target is globally stable conditional on a regime. A regime switch changes the target and the convergence speed immediately, while territory itself remains continuous.

This result gives a precise interpretation of regime switching. Fatigue can jump between strategic regimes only when a boundary is reached or a threshold is crossed, but the territorial state adjusts smoothly toward the new target.

4.4 Fatigue thresholds and coexistence under state dependence

For each regime R, define the stationary efforts

$$g_i^R := g_i^R(x_R^*), \qquad g_j^R := g_j^R(x_R^*).$$

The fatigue roots conditional on regime R are

$$c_{i,R}^{\pm} = \frac{1 \pm \sqrt{1 + 4(g_i^R - k)}}{2}, \tag{4.23}$$

whenever the discriminant is nonnegative, with analogous expressions for j.

Proposition 11 (Regime consistency with state dependence)**.** *A state-dependent stationary regime profile R is fatigue-consistent if the following conditions hold for each player:*

$$R_i = \mathrm{B} \Longrightarrow k \geq g_i^R, \tag{4.24}$$

$$R_i = \mathrm{I} \Longrightarrow k < g_i^R + \frac{1}{4}. \tag{4.25}$$

The corresponding conditions apply to player j.

All four regime profiles are simultaneously fatigue-consistent whenever

$$\begin{aligned} \max\left\{g_i^{\mathrm{BI}}, g_i^{\mathrm{BB}}, g_j^{\mathrm{IB}}, g_j^{\mathrm{BB}}\right\} &\leq k \\ &< \min\left\{g_i^{\mathrm{II}} + \frac{1}{4}, g_j^{\mathrm{II}} + \frac{1}{4}, g_j^{\mathrm{BI}} + \frac{1}{4}, g_i^{\mathrm{IB}} + \frac{1}{4}\right\}. \end{aligned} \tag{4.26}$$

Whenever this interval is nonempty, the model admits four distinct stationary-regime outcomes with different fatigue stocks, efforts, and territorial shares.

Unlike the state-independent exponential contest, regime changes now modify both players' effort choices. A switch by player j from I to B changes a_j, shifts x_R^*, changes g_i^R, and therefore moves player i's fatigue threshold. Coexistence is no longer merely player-by-player; it is a property of the entire regime profile.

4.5 State-dependent dynamic reversal

The coexistence of different fatigue regimes raises a natural question: can a player that initially enjoys a territorial advantage eventually lose its majority because its opponent recovers from fatigue? Unlike the state-independent contest, where reversal concerns the instantaneous probability of success, territorial state dependence allows changes in relative fighting incentives

to translate into persistent changes in territorial control. The key mechanism is that recovery modifies the regime-specific marginal effort wedges and, consequently, the stationary territorial allocation.

Consider two players with $\rho_i < \rho_j$, so that player i is less vulnerable to fatigue. When both players remain in the interior regime, this asymmetry favors player i. However, if player j reaches the fatigue boundary while player i remains interior, the relative ranking of their marginal effort wedges is reversed. The following proposition characterizes the resulting change in territorial control.

Proposition 12 (Territorial reversal after a fatigue switch)**.** *Suppose $\rho_i < \rho_j$ and consider the admissible stationary configurations* (I,I) *and* (I,B)*, with strictly positive efforts.*

In the interior–interior regime,

$$x^*_{\mathrm{II}} > \frac{1}{2}. \tag{4.27}$$

When player j reaches the fatigue boundary while player i remains interior, the post-switch stationary territorial target satisfies

$$x^*_{\mathrm{IB}} < \frac{1}{2}. \tag{4.28}$$

Consequently,

$$x^*_{\mathrm{II}} > \frac{1}{2} > x^*_{\mathrm{IB}}. \tag{4.29}$$

Under the piecewise-stationary adjustment rule, suppose that the switch to (I,B) *occurs at time τ and that this regime persists thereafter. If $x_i(\tau) > 1/2$, the territorial share of player i crosses $1/2$ in finite time and subsequently converges to $x^*_{\mathrm{IB}} < 1/2$.*

The proposition reveals that the initial advantage associated with lower fatigue vulnerability need not translate into long-run territorial dominance. When both players are fatigued, player i benefits from its lower marginal burden of effort and controls the larger stationary territorial share. Once player j recovers, however, its fatigue-related wedge disappears, while player i continues to bear the shadow cost of fatigue. The player that was initially disadvantaged may therefore become the long-run majority controller, despite remaining structurally more vulnerable to fatigue.

Importantly, the reversal of stationary territorial targets does not imply an immediate reversal of actual territorial control. Military effort adjusts when the fatigue regime changes, and the instantaneous probability of success may respond immediately. Territory, by contrast, is a predetermined state variable that retains the effects of past contest outcomes. Under a persistent (I,B) regime, it gradually converges toward the new stationary target. Thus, the underlying balance of strategic advantage can change before the territorial distribution reflects that change.

This mechanism differs from the pre-boundary equilibrium reversal established in Section 3, where optimal effort adjusts continuously along the recovery path. Here, territorial reversal follows a change in the stationary configuration and is characterized under the piecewise-stationary adjustment rule. Whether the asymmetric regime persists or triggers a further recovery event is examined in the next subsection.

4.6 Switching cascades

A first fatigue switch can either produce a persistent asymmetric regime or initiate a second switch.

Proposition 13 (Post-switch cascade criterion)**.** *Suppose the system initially follows the* (I,I) *regime and player* j *reaches the fatigue boundary at time* τ*, while* $c_i(\tau) > 0$*. Under piecewise-stationary adjustment, the post-switch candidate is* (I,B)*, with stationary efforts* g_i^{IB} *and* g_j^{IB}*. Assume that player* j*'s boundary is viable,* $k \geq g_j^{\mathrm{IB}}$*.*

The subsequent fatigue dynamics of player i *satisfy the following classification.*

(i) If $k \leq g_i^{\mathrm{IB}}$*, player* i *cannot recover to the boundary and converges to a positive high-fatigue steady state.*

(ii) If

$$g_i^{\mathrm{IB}} < k < g_i^{\mathrm{IB}} + \frac{1}{4},$$

the unstable threshold is

$$c_{i,\mathrm{IB}}^{-} = \frac{1 - \sqrt{1 + 4(g_i^{\mathrm{IB}} - k)}}{2}.$$

If $c_i(\tau) < c_{i,\mathrm{IB}}^{-}$*, player* i *reaches the fatigue boundary in finite time. If* $c_i(\tau) > c_{i,\mathrm{IB}}^{-}$*, it converges to the positive high-fatigue steady state. At equality,* $c_i(\tau) = c_{i,\mathrm{IB}}^{-}$*, fatigue remains at the unstable stationary threshold.*

(iii) If $k = g_i^{\mathrm{IB}} + \frac{1}{4}$*, player* i *reaches the boundary when* $c_i(\tau) < 1/2$*. For* $c_i(\tau) \geq 1/2$*, fatigue instead remains at or converges asymptotically to* $1/2$*.*

(iv) If $k > g_i^{\mathrm{IB}} + \frac{1}{4}$*, player* i *reaches the fatigue boundary in finite time for every finite* $c_i(\tau) > 0$*.*

Whenever player i *reaches the boundary, a persistent transition to* (B,B) *is supported provided that*

$$k \geq \max\{g_i^{\mathrm{BB}}, g_j^{\mathrm{BB}}\}.$$

Otherwise, reaching the boundary does not by itself guarantee persistence of the (B,B) *regime.*

The symmetric statements apply when player i reaches the boundary first.

A first recovery event may therefore lead either to a persistent asymmetric regime or to a second recovery event. When the latter produces a viable (B, B) regime, the long-run territorial target returns to the symmetric share $x_i^* = 1/2$. By contrast, a persistent asymmetric regime favors the player that has reached the fatigue boundary. Thus, the long-run territorial consequences of recovery depend on whether the initial switch induces a subsequent, sustainable transition of the opponent.

4.7 Economic mechanisms and strategic feedbacks

The introduction of territorial state dependence enriches the fatigue mechanism through several interconnected economic channels. Unlike the separable contest, in which each player's optimal effort is independent of the opponent's choices, the marginal effectiveness of military effort now depends on the existing territorial distribution. As shown in (4.3), player i's marginal return to effort is proportional to the territory not yet controlled, $1 - x_i$, whereas player j's marginal return is proportional to x_i. Hence, controlling a larger territorial share does not necessarily strengthen a player's incentives to exert additional effort: it also reduces the territory left to gain and increases the share exposed to the opponent. Moreover, since current success affects future territorial control, effort has an intertemporal value reflected in the territorial shadow values.

A second mechanism concerns the interaction between fatigue status and relative strategic advantage. Within a stationary regime, the effective marginal burden of effort is summarized by the wedge a_i^R. When both players remain in the interior, the less fatigue-vulnerable contestant faces the smaller wedge and, under the admissible stationary configuration, controls the larger territorial share. However, if the more vulnerable player j reaches the fatigue boundary while i remains interior, its wedge falls from $1 + \rho_j$ to 1, becoming smaller than $1 + \rho_i$. Consequently, the stationary territorial ranking reverses, as established in Proposition 12. The relevant advantage is therefore not determined by fatigue vulnerability alone, but also by the fatigue regime reached along the adjustment process.

Importantly, a change in the stationary territorial ranking does not imply an instantaneous transfer of territory. Under the piecewise-stationary adjustment rule, a regime switch changes the effort configuration and the associated territorial target, while the inherited territorial stock remains continuous. The instantaneous success probability may respond immediately to the revised efforts, whereas actual territorial control adjusts gradually toward the new target, according to Proposition 10. A contestant may therefore lose its probability advantage before losing its territorial majority. This distinction captures the inertia of accumulated territorial

control: past success continues to influence the observed distribution of territory even after the underlying strategic configuration has changed.

State dependence also creates a feedback from one player's recovery to the opponent's fatigue dynamics. Because the stationary effort configuration depends on both players' regime wedges and on the associated territorial target, the recovery of player j can alter player i's effort even when i's own fatigue stock is unchanged at the switching date. In particular, if the switch raises g_i^R, the unstable fatigue threshold of player i decreases whenever the corresponding recovery basin exists. A fatigue stock that previously belonged to the recovery basin may consequently lie above the new threshold. Thus, the opponent's recovery can interrupt an ongoing recovery process and redirect player i toward persistent high fatigue, without any direct shock to its fatigue stock. This is the mechanism of switching-induced trapping illustrated in Section 5.

The same interaction can also generate switching cascades. Depending on the fatigue stocks at the first switching date and on the resulting regime-specific efforts, the opponent may either remain in a high-fatigue regime or subsequently reach the boundary. A persistent asymmetric regime favors the player that has recovered, whereas a subsequent transition to a viable (B, B) regime restores the symmetric stationary territorial target. The order and timing of recovery events therefore matter for the long-run distribution of territory.

These mechanisms therefore reveal how territorial outcomes inherit the path dependence generated by fatigue. Conditional on a fixed regime and its stationary efforts, territorial adjustment has a unique stable target. Different long-run territorial outcomes arise instead because initial fatigue stocks and the sequence of recovery events select different regime configurations.

5 Numerical illustrations of regime selection and strategic reversal

This section uses the closed-form stationary regimes to illustrate the transition mechanisms emphasized by the analytical results. The purpose of the exercises is not to calibrate a particular conflict. Instead, the parameter configurations are selected to isolate economically distinct phenomena: fatigue bistability, a reversal in success probabilities, territorial reversal, an endogenous change in an opponent's basin of attraction, and global path dependence across the four fatigue regimes.

5.1 Numerical solution concept and computational protocol

A qualification is important. In the state-dependent model, equations (4.8)–(4.9) characterize stationary controls associated with a fatigue regime and its stationary territorial target. They are not, by themselves, the complete nonstationary feedback strategies of a Markov-perfect equilibrium. The numerical exercises therefore implement the same *piecewise-stationary adjustment* concept used in the theoretical discussion.

For each regime

$$R \in \{(\mathrm{I},\mathrm{I}), (\mathrm{B},\mathrm{I}), (\mathrm{I},\mathrm{B}), (\mathrm{B},\mathrm{B})\},$$

the algorithm proceeds as follows.

(i) It computes the regime-specific wedges a_i^R and a_j^R.

(ii) In the state-dependent model, it obtains the unique economic root $x_R^* \in (0,1)$ of (4.10). Numerically, the fixed-point residual in (B.14) is solved by a bracketed root-finding method. This is numerically more stable than direct evaluation of Cardano's formula.

(iii) It computes the stationary controls g_i^R and g_j^R, and verifies the interior-effort restrictions

$$0 < \mathrm{e}^{-g_i^R} < 1, \qquad 0 < \mathrm{e}^{-g_j^R} < 1.$$

(iv) Conditional on the current regime, the controls are held fixed and the state equations are integrated. Fatigue follows the projected law (2.7). In the state-dependent model, territory follows (4.2).

(v) When an interior fatigue stock reaches zero, the corresponding player switches from I to B. The controls and the territorial target are recomputed for the new regime. Fatigue and territory are continuous at the switching date, whereas the controls and the success probability may jump.

(vi) A boundary regime is retained only when it is viable:

$$g_i^R \le k \quad \text{for every player } i \text{ with } R_i = \mathrm{B}.$$

Within a fixed state-dependent regime, the territorial law is linear. Consequently, the numerical integration reproduces the closed-form transition in Proposition 10. The event-driven procedure is needed only to identify the time at which a fatigue boundary is reached and the regime-specific controls change.

Table 1: Parameter configurations used in the numerical illustrations

Experiment	Model	π	ρ_i	ρ_j	k	$c_i(0)$	$c_j(0)$	$x_i(0)$
1	Reduced fatigue dynamics	8	0.10	–	1.45	multiple	–	–
2	Exponential, state independent	3	0.05	0.25	0.42	0.20	0.10	–
3	Exponential, state dependent	4	0.349494	0.926178	0.36	0.50	0.20	x^*_{II}
4	Exponential, state dependent	4	0.349494	0.926178	0.36	0.25	0.05	x^*_{II}
5	Exponential, state dependent	3.25	0.248101	0.657943	0.286028	grid	grid	–

Table 1 reports the parameter configurations. The relatively precise values in Experiments 3–5 are deliberately retained to make the figures exactly reproducible. They are not estimates.

5.2 Fatigue bistability and threshold dependence

The first exercise isolates the fatigue mechanism from strategic interaction. We use the state-independent interior effort associated with

$$\pi = 8, \qquad \rho = 0.10,$$

which gives

$$g = \ln\left(\frac{8}{2(1.10)}\right) \simeq 1.2910.$$

With $k = 1.45$, the model lies in the bistability region:

$$g < k < g + \frac{1}{4}.$$

The two interior stationary fatigue stocks are

$$c^- \simeq 0.1984, \qquad c^+ \simeq 0.8016.$$

Figure 1 displays both the phase portrait and the corresponding transition paths. Panel (a) plots

$$\dot{c} = g + c - c^2 - k.$$

The drift is negative on $(0, c^-)$, positive on (c^-, c^+), and negative above c^+. Under the projected law, zero is absorbing. Hence c^- is the separatrix between full recovery and persistent high fatigue.

Panel (b) starts the system from

$$c(0) \in \{0.04, 0.12, 0.19, 0.30, 0.70, 1.05\}.$$

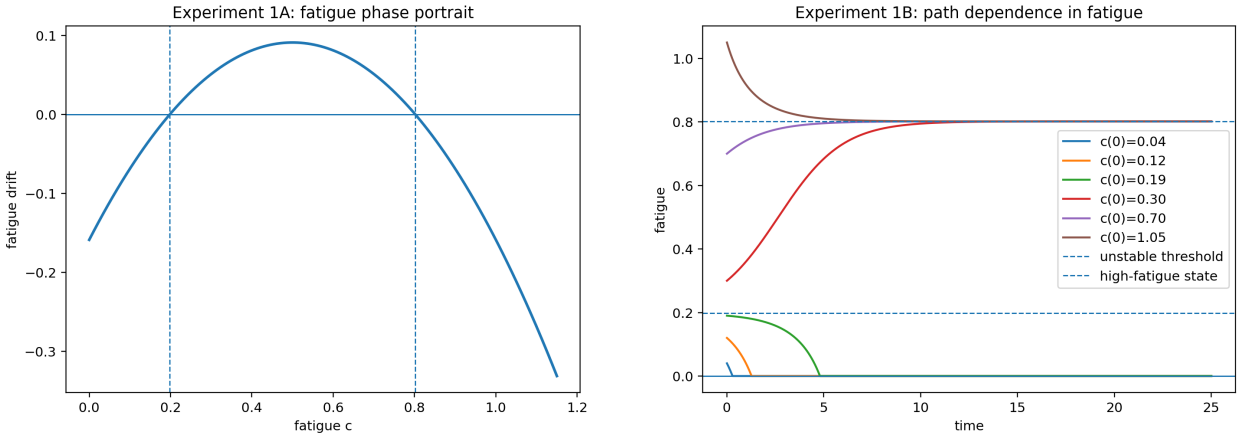

(a) Fatigue drift and stationary points.

(b) Transition paths from different initial conditions.

Figure 1: Bistability and path dependence in the fatigue state.

The first three paths reach the boundary, whereas the remaining paths converge to c^+. The exercise makes clear that the high-fatigue outcome is not caused by an unusually large instantaneous shock alone. What matters is whether the state lies above the endogenous threshold. Two initially close fatigue stocks can therefore generate permanently different outcomes.

The same picture also clarifies the comparative statics in Proposition 5. An increase in equilibrium effort shifts the fatigue parabola upward, lowers c^-, and enlarges the basin of the high-fatigue state. Military aggressiveness is therefore beneficial in the contest but harmful for recovery.

5.3 Verified equilibrium recovery and pre-boundary reversal

We consider the parameter configuration

$$\pi = 3, \qquad \rho_i = 0.05, \qquad \rho_j = 0.25, \qquad k = 0.42, \qquad c_i(0) = 0.20, \quad c_j(0) = 0.10.$$

Both players satisfy the strict coexistence conditions (3.26), and the stationary interior efforts and thresholds are

$$g_i^{\mathrm{I}} \simeq 0.356675, \quad g_j^{\mathrm{I}} \simeq 0.182322, \quad g^{\mathrm{B}} \simeq 0.405465, \quad c_i^- \simeq 0.067941, \quad c_j^- \simeq 0.388997.$$

Player i starts above its threshold and therefore optimally holds g_i^{I} at all dates; its fatigue converges to the high root. Player j starts below its threshold. Its HJB-optimal effort,

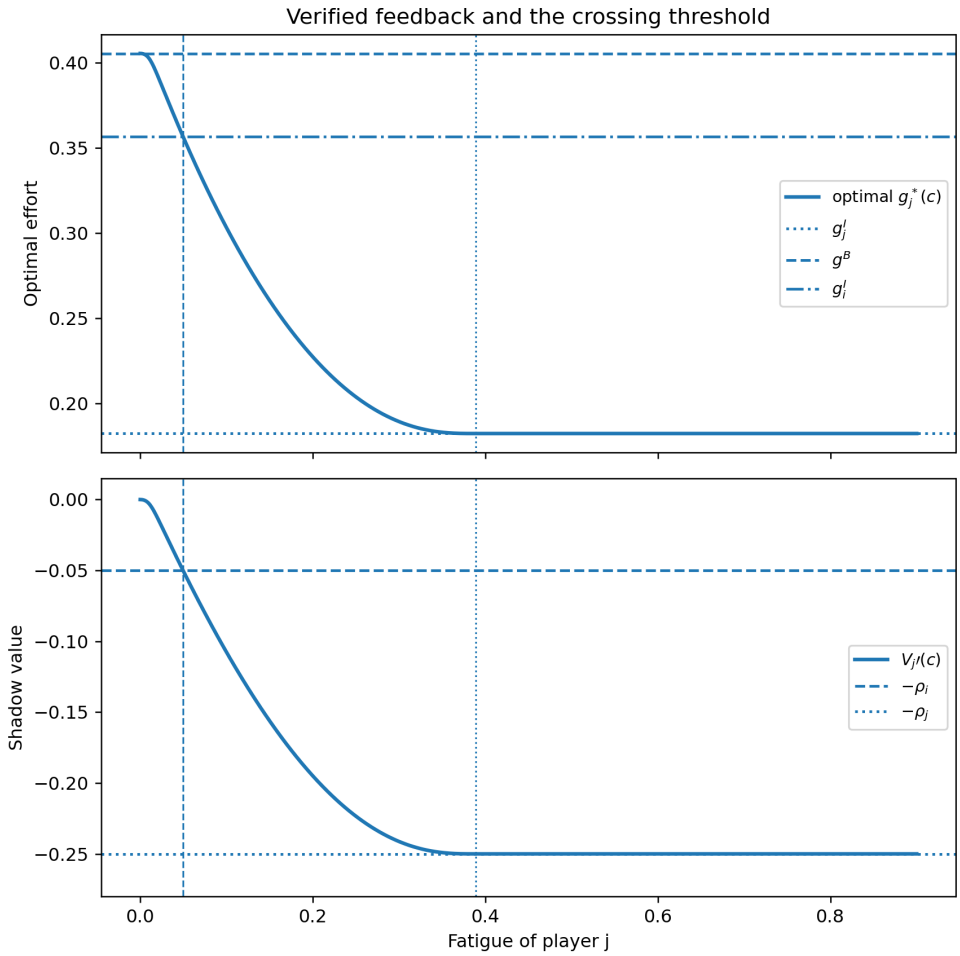

Figure 2: Globally verified optimal feedback and shadow value for player j. The vertical lines mark the effort-crossing stock $c_{j,\times}$ and the optimal recovery threshold c_j^-.

however, is *not* g_j^{I} until the boundary: the verified feedback begins at

$$g_j^*(0.10) \simeq 0.303163$$

and increases continuously toward g^{B} as fatigue falls. Figure 2 plots both the shadow value $V_j'(c)$ and the associated optimal feedback. The critical effort-crossing state satisfies

$$\ell_j(c_{j,\times}) = -\rho_i = -0.05, \qquad c_{j,\times} \simeq 0.049593.$$

Thus $c_j(0) > c_{j,\times}$ and the initial ranking is $g_i^*(0) > g_j^*(0)$, with $p_i(0) \simeq 0.519239 > 1/2$.

The equilibrium trajectories in Figure 3 produce a success-probability reversal at

$$t_\times \simeq 2.34208,$$

whereas player j reaches $c_j = 0$ only at

$$T_j \simeq 7.32587.$$

The player j therefore becomes the more aggressive contestant approximately 4.98 time units *before* completing recovery. The limiting probability still satisfies $p_i^{\mathrm{IB}} = 1/2 - \rho_i/\pi \simeq 0.483333$, but the adjustment is *smooth and anticipatory*.

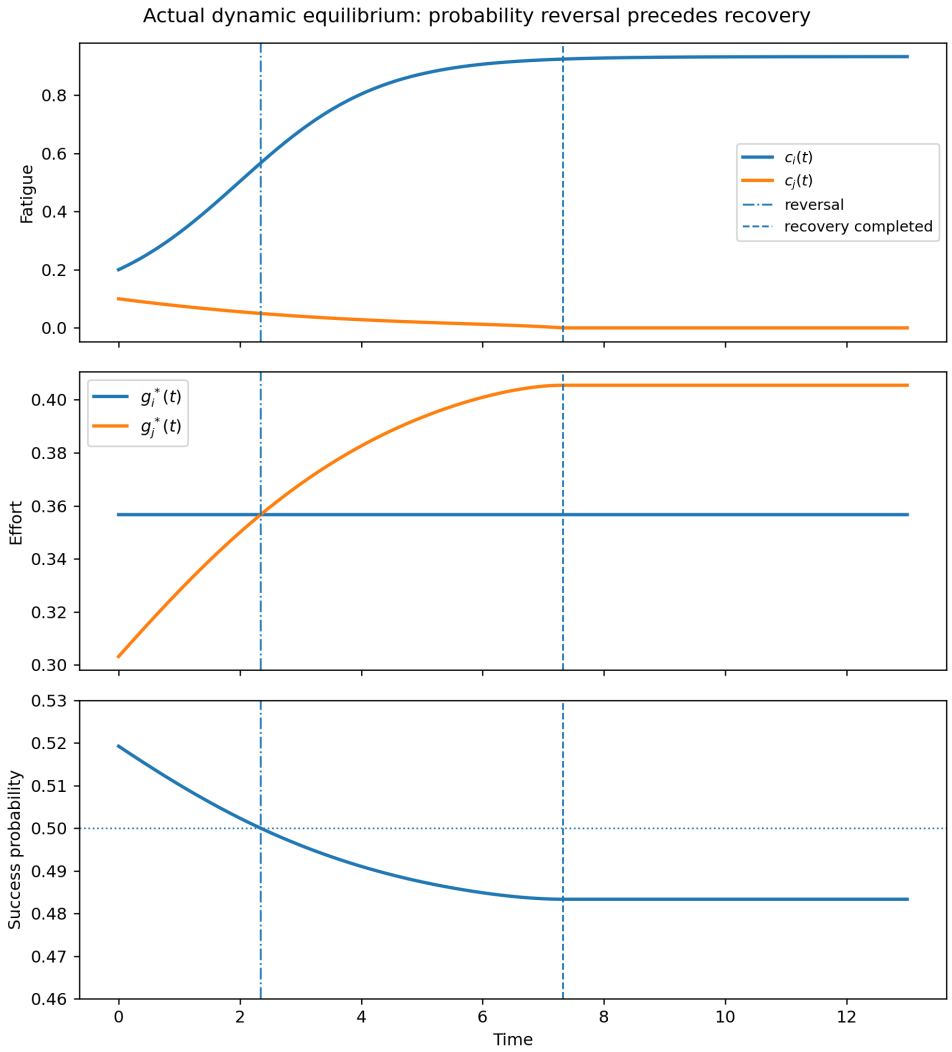

Figure 3: Verified state-independent Nash transition. The dash-dot line is the *pre-boundary* probability reversal; the dashed line is completion of player j's recovery.

Figure 4 compares the equilibrium path with a piecewise-stationary benchmark, in which effort is held at its regime-specific stationary value until the boundary is reached. Under this benchmark, recovery would be completed at $T_j^{\mathrm{PS}} \simeq 0.53345$ and effort would jump abruptly

from g_j^{I} to g^{B}. This path is not optimal. Removing the opponent-dependent additive payoff, its discounted value is 0.082997, against the HJB-optimal value 0.089510. Even the constant policy $g_j(t) = 0.33$, which maintains $c_j(t) = 0.10$, yields 0.089114 and is thus a strictly profitable deviation from the benchmark. Anticipation of recovery is therefore an essential feature of optimal behavior. In this example the benchmark selects the same long-run regime as the optimal policy, but it misrepresents the timing and shape of the transition. No analogous comparison is available for the state-dependent model, for which we have not derived optimal feedback strategies. The transitions and the regime selection reported in Subsections 5.4–5.6 are accordingly conditional on the piecewise-stationary adjustment rule.

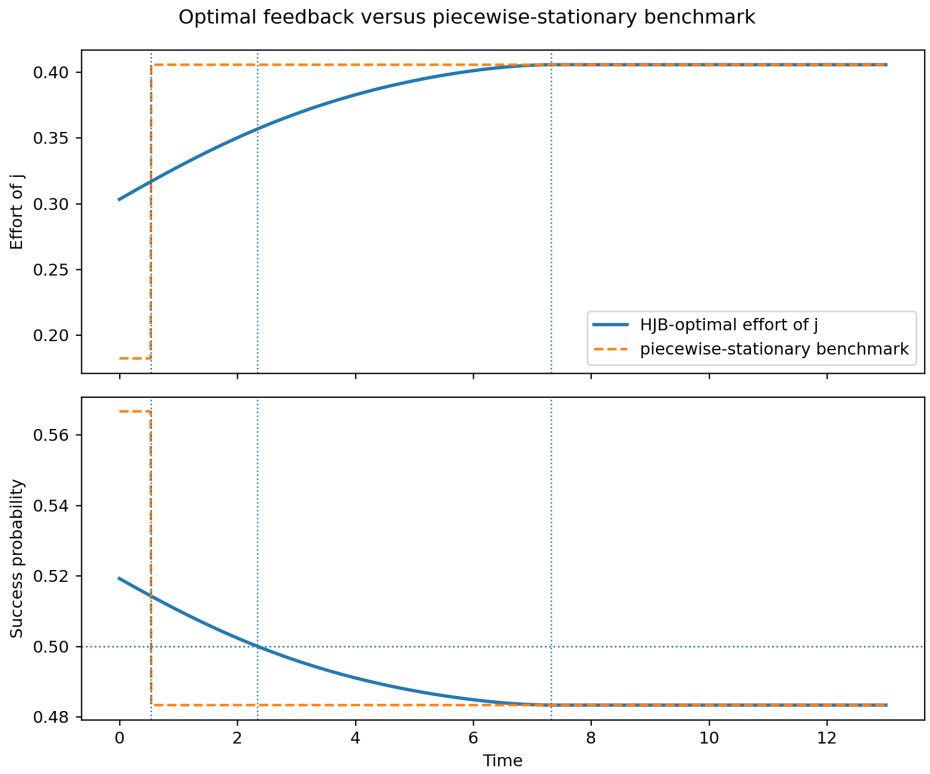

Figure 4: Piecewise-stationary benchmark (dashed) versus verified optimal feedback (solid). The benchmark is not an equilibrium path.

Figure 5 compares the verified value function with the global linear bound $A_j - \rho_j c$. The bound is attained in the high-fatigue region and is strictly above the value of every recovery state. Figure 6 then varies ρ_j while holding ρ_i, π, and k fixed, and plots the nonempty interval $c_{j,\times} < c_j(0) < c_j^-$ that guarantees an initially positive advantage for i followed by a reversal *before* recovery. This is a numerical depiction of the open-set assertion in Proposition 7.

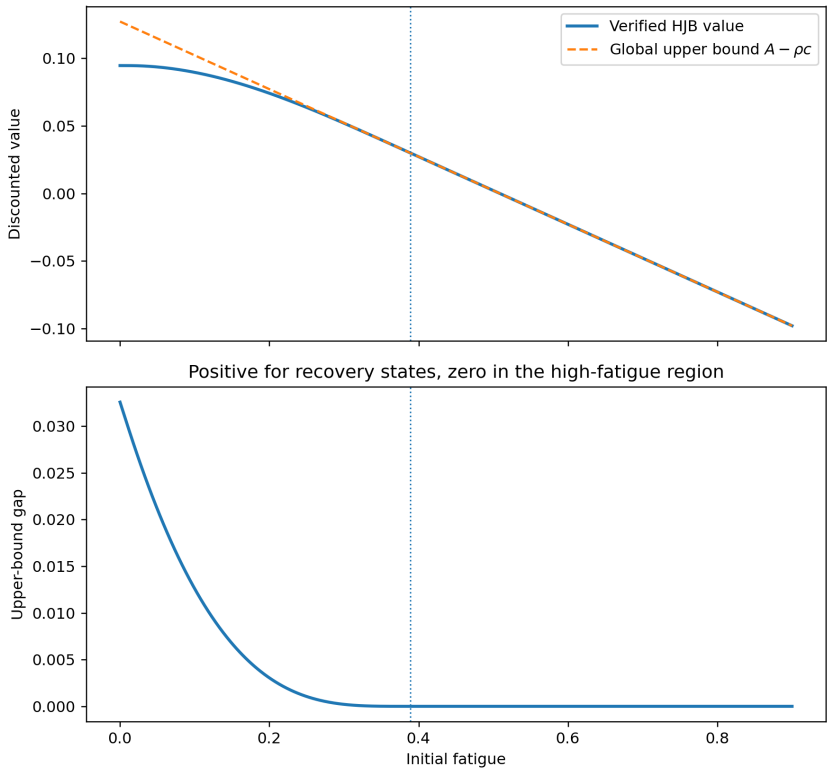

Figure 5: Verified discounted value and the global bound. Equality holds exactly in the high-fatigue region, while the recovery branch lies strictly below the bound.

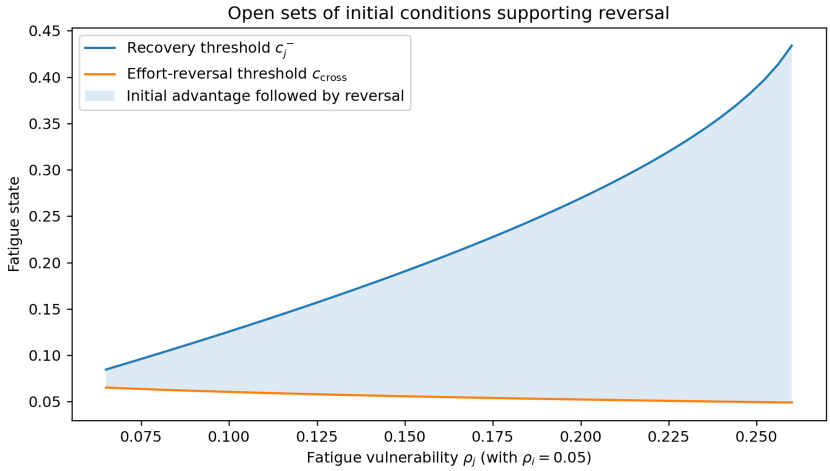

Figure 6: Robustness of pre-boundary reversal to vulnerability ρ_j. The shaded interval contains fatigue initial conditions that support an initially stronger player i and a later equilibrium reversal.

5.4 State dependence: effort, probability, and territorial reversal

We now turn to the state-dependent model. Let

$$\pi = 4, \qquad \rho_i = 0.349494, \qquad \rho_j = 0.926178, \qquad k = 0.36.$$

Again, player i is less vulnerable to fatigue. In the (I, I) regime, the stationary solution is

$$x^*_{\mathrm{II}} \simeq 0.5794, \qquad g_i^{\mathrm{II}} \simeq 0.1244, \qquad g_j^{\mathrm{II}} \simeq 0.0888. \tag{5.1}$$

Thus player i begins as the majority territorial controller and exerts more effort than player j.

We initialize territory at $x_i(0) = x^*_{\mathrm{II}}$ and set

$$c_i(0) = 0.50, \qquad c_j(0) = 0.20.$$

For player i,

$$c^-_{i,\mathrm{II}} \simeq 0.3800 \quad \text{and} \quad c^+_{i,\mathrm{II}} \simeq 0.6200,$$

so i is in the high-fatigue basin. For player j,

$$k > g_j^{\mathrm{II}} + \frac{1}{4}.$$

The interior fatigue roots do not exist and j's fatigue drift is negative for every $c_j \geq 0$. Hence player j necessarily reaches the boundary. The switching date is

$$\tau \simeq 1.1568.$$

After the switch, the relevant regime is (I, B). Its stationary solution is

$$x^*_{\mathrm{IB}} \simeq 0.4449, \qquad g_i^{\mathrm{IB}} \simeq 0.2654, \qquad g_j^{\mathrm{IB}} \simeq 0.3437. \tag{5.2}$$

Figure 7 traces the consequences of this switch for fatigue, effort, and territorial control. Its three panels show how a recovery that concerns player j alone is transmitted to both contestants.

First, as Panel (b) shows, recovery by one player leads to escalation by both, but for different reasons. For player j, the disappearance of the fatigue shadow cost lowers the marginal burden of effort from $1 + \rho_j$ to one: fighting becomes cheaper. Player i's burden is unchanged. Its stationary effort rises because, in the new configuration, it controls less

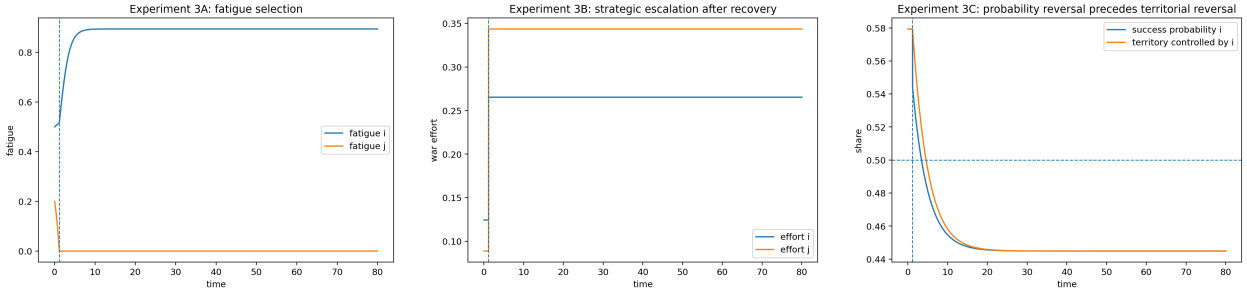

(a) Fatigue-regime selection. (b) Reversal of the effort ranking. (c) Probability leads territory.

Figure 7: State-dependent reversal. Player j's transition to the boundary changes both controls and moves the territorial target from $x^*_{\mathrm{II}} > 1/2$ to $x^*_{\mathrm{IB}} < 1/2$.

territory and therefore has more to regain: the term $1 - x^*_R$ in its marginal return increases from 0.4206 to 0.5551. This effect outweighs the fall in the marginal value of current success, inclusive of its territorial continuation value (B.10), from 7.27 to 6.34. As both sides fight harder, current territorial gains become less persistent and hence less valuable. Player i thus escalates out of a weaker position, whereas j escalates out of a renewed capacity to fight. The latter response is stronger, and the effort ranking reverses:

$$g_i^{\mathrm{II}} > g_j^{\mathrm{II}} \quad \text{but} \quad g_i^{\mathrm{IB}} < g_j^{\mathrm{IB}}.$$

Second, the long-run territorial target moves from a majority for i to a minority:

$$x^*_{\mathrm{II}} \simeq 0.5794 \quad \longrightarrow \quad x^*_{\mathrm{IB}} \simeq 0.4449.$$

This is the numerical counterpart of Proposition 12. The player with the lower structural vulnerability to fatigue becomes the minority controller because what governs relative incentives is the burden of fatigue that is currently active: a highly vulnerable player that has recovered faces a lower marginal cost of fighting than a resilient player that is still fatigued.

Third, Panel (c) shows that the balance of effort, the balance of success, and the balance of territory reverse in sequence. At τ, player j becomes the more aggressive contestant, yet i's success probability only falls from 0.5794 to approximately 0.5441. Two forces cushion the decline. The inherited majority still favors i, and i's own escalation offsets part of j's: had only j's effort changed, the probability would have fallen to 0.5197. The protection is temporary. Since p_i is now below x_i, territory is eroded according to

$$\dot{x}_i = p_i - x_i,$$

and this erosion further reduces the probability of success. The latter falls below one half at $t \simeq 3.402$, whereas territory crosses one half only at $t \simeq 4.561$. Between these dates player i still holds most of the territory although it is already more likely to lose than to win. The map of territorial control, a stock that records past success, is thus a lagging indicator of military advantage.

Fourth, Panel (a) reveals the cost of this escalation. Player i is already in the high-fatigue basin, so the switch does not alter the type of regime to which it converges, but it makes that regime considerably more burdensome. The high-fatigue target moves from approximately 0.6200 to

$$c^{+}_{i,\mathrm{IB}} \simeq 0.8942,$$

and, because the cost of fatigue is convex, the associated flow cost $\rho_i c_i^2$ more than doubles, from 0.134 to 0.279. The opponent's recovery therefore harms player i twice: i ends up spending more on the conflict, in both effort and fatigue, while controlling less territory.

The economic message of Figure 7 is that greater effort need not signal greater strength, nor does a territorial majority guarantee a continuing advantage. An observer looking at player i shortly after τ would see higher military effort and a majority of territory, although the conflict has already entered a regime in which that majority cannot be sustained. The different speeds at which effort, success, and territory adjust can thus conceal a strategic reversal until well after its cause, the opponent's recovery, has materialized.

5.5 Switching-induced trapping: when the opponent's recovery destroys one's own recovery

The next experiment uses the same primitives as the previous one but changes the initial fatigue stocks:

$$c_i(0) = 0.25, \qquad c_j(0) = 0.05.$$

The initial fatigue of player i satisfies

$$c_i(0) = 0.25 < c^{-}_{i,\mathrm{II}} \simeq 0.3800.$$

Before any regime switch, player i is therefore recovering:

$$\dot{c}_i < 0.$$

Player j, whose fatigue drift is globally negative in the (I,I) regime, reaches zero quickly, at

$$\tau \simeq 0.2030.$$

At that date,

$$c_i(\tau) \simeq 0.2397.$$

The switch from (I,I) to (I,B) raises player i's effort from

$$g_i^{\mathrm{II}} \simeq 0.1244$$

to

$$g_i^{\mathrm{IB}} \simeq 0.2654.$$

Because the unstable fatigue threshold is decreasing in effort, player i's threshold falls from

$$c_{i,\mathrm{II}}^{-} \simeq 0.3800$$

to

$$c_{i,\mathrm{IB}}^{-} \simeq 0.1058.$$

The state at the switching date consequently satisfies

$$c_{i,\mathrm{IB}}^{-} < c_i(\tau) < c_{i,\mathrm{II}}^{-}. \tag{5.3}$$

Condition (5.3) is the core of the mechanism illustrated in Figure 8. The two horizontal lines in Panel (a) are player i's thresholds before and after the switch. The same fatigue stock lies in the recovery basin under the former and in the high-fatigue basin under the latter. The fatigue path therefore changes direction at the switching date: it declines before τ, reaches its minimum at approximately 0.2397, and then rises toward

$$c_{i,\mathrm{IB}}^{+} \simeq 0.8942.$$

Had the pre-switch efforts remained in place, player i would instead have recovered fully at $t \simeq 2.319$. What player i loses is thus a recovery that was already under way. No shock hits its fatigue stock, its vulnerability, or its replenishment capacity; the only event is the opponent's recovery.

Panel (b) identifies the channel. Replenishment k is the same before and after the switch, but the additional effort absorbs the margin $k - g_i$ that made recovery possible, which

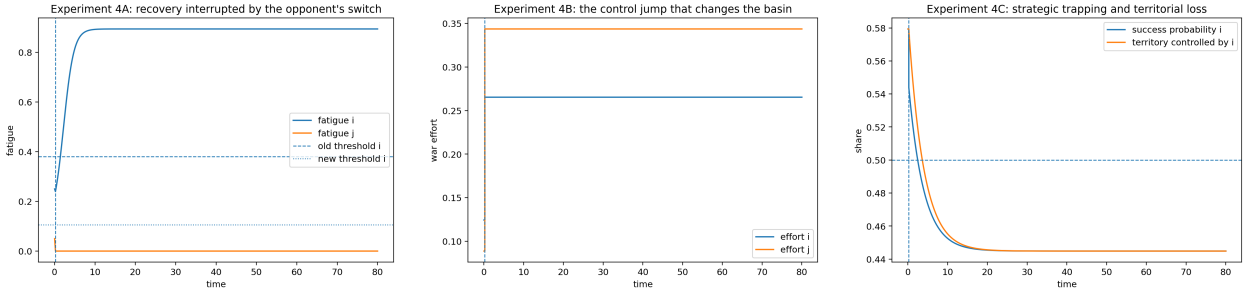

(a) A recovery path turns into high fatigue.

(b) The control jump shifts the threshold.

(c) The associated strategic and territorial loss.

Figure 8: Switching-induced trapping. Recovery by player j raises player i's effort, shrinks i's recovery basin, and reverses the direction of i's fatigue path.

shrinks from 0.2356 to 0.0946. At the current fatigue stock this margin no longer offsets the self-reinforcing component of fatigue, $c_i - c_i^2 \simeq 0.1823$. In economic terms, resources that would have restored fighting capacity are diverted to current fighting. Panel (c) shows what this diversion buys and what it does not. The higher effort softens the immediate fall in i's success probability, but it does not preserve the initial advantage: the probability falls below one half at $t \simeq 2.448$ and territory follows at $t \simeq 3.608$. Escalation provides temporary protection on the battlefield at the price of persistent exhaustion.

This phenomenon is absent from the separable state-independent exponential contest. There, player i's stationary effort depends only on i's own fatigue regime, so a switch by j cannot move i's threshold. State dependence creates a *regime-mediated strategic externality*: one player's recovery changes the other's control and can destroy the other's recovery path without any direct shock to that player's fatigue stock.

The comparison between Figures 7 and 8 clarifies why this result is stronger than a conventional reversal in contest success. Primitives, post-switch efforts, and long-run territorial shares are identical in the two experiments; only initial fatigue differs. In the former, the opponent's recovery operates on an *intensive margin*, deepening the exhaustion of a player that would have remained fatigued in any case. In the latter, it operates on an *extensive margin*, moving the player from one basin of attraction to another and eliminating its recovery altogether. Identical territorial losses may therefore conceal very different opportunity costs. An earlier recovery is valuable to player j not only because it raises j's own fighting capacity, but also because it can close the opponent's window for recovery.

This interpretation is conditional on the adjustment rule. At τ, player i's effort is set at the stationary value associated with the new territorial target, although territory has not yet adjusted, and this response need not be optimal along the transition. Switching-induced trapping should accordingly be read as a property of piecewise-stationary adjustment, rather

Table 2: Stationary regime outcomes in the basin-map experiment

Regime	x_R^*	g_i^R	g_j^R
(I, I)	0.5666	0.0660	0.0501
(B, I)	0.6117	0.1347	0.0834
(I, B)	0.4548	0.1822	0.2227
(B, B)	0.5000	0.2719	0.2719

than as a prediction of equilibrium behavior.

5.6 Global basin maps and long-run territorial path dependence

The previous exercises selected particular initial conditions. We now vary both fatigue stocks over a grid and identify the final regime under the piecewise-stationary adjustment rule. The parameters are

$$\pi = 3.25, \qquad \rho_i = 0.248101, \qquad \rho_j = 0.657943, \qquad k = 0.286028.$$

For this configuration, every boundary effort is weakly below k, and all four regime profiles are viable. Their stationary outcomes are reported in Table 2.

The grid is

$$(c_i(0), c_j(0)) \in [0.001, 0.80]^2,$$

with 120 points along each dimension. The classification uses the exact constant-effort hitting times from (3.17). If one player reaches zero first, the algorithm recomputes the other player's effort and then evaluates whether the remaining player reaches the boundary under the new regime.

Panel (a) of Figure 9 maps initial fatigue into the final regime. The regions are not simple Cartesian products of two independent one-player basins. Their boundaries bend because the identity and timing of the first player to recover matter. The first switch changes both controls and can either prevent or induce a second switch.

At the displayed grid resolution, approximately 31.1% of the grid leads to (I, I), 24.6% to (B, I), 34.3% to (I, B), and 10.0% to (B, B). These percentages are descriptive properties of the plotted rectangle rather than structural probabilities. Their value is to show that none of the four outcomes is a knife-edge event under this parameter configuration.

Panel (b) maps each final regime into its stationary territorial target. The same primitives can produce

$$x_i^* > 0.5, \qquad x_i^* < 0.5, \qquad \text{or} \qquad x_i^* = 0.5$$

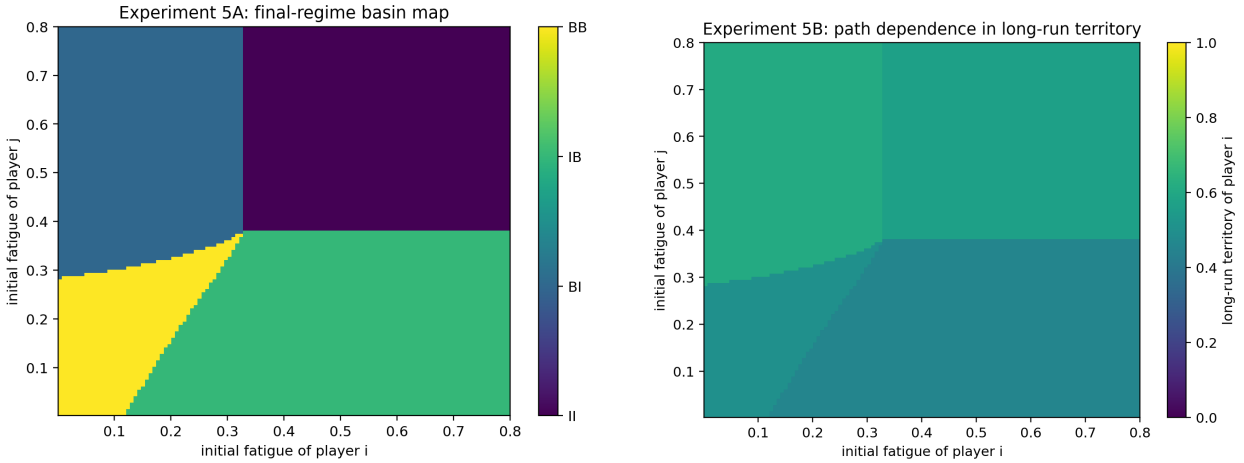

(a) Final fatigue regime.

(b) Long-run territorial target.

Figure 9: Global path dependence. Initial fatigue determines the order of switches, the final regime profile, and the identity of the long-run majority controller.

solely because the initial fatigue stocks differ. In particular, a small change in initial fatigue near a basin boundary can reverse the identity of the majority territorial controller. Initial fatigue is therefore not a transitory nuisance: through regime selection, it has permanent territorial consequences.

5.7 Synthesis of the numerical mechanisms

Taken together, the exercises reveal four distinct channels.

First, nonlinear fatigue creates *within-player path dependence*. A player below the unstable threshold recovers; a player above it remains fatigued.

Second, reaching the boundary creates a *strategic reversal*. The boundary player eliminates the fatigue shadow wedge and may become the more aggressive and more successful contestant.

Third, state dependence creates a separation between *controls*, *success probabilities*, and *territory*. Controls jump at a regime change, probabilities react immediately but remain conditional on inherited territory, and territory adjusts continuously.

Fourth, state dependence creates *cross-player basin effects*. A regime switch by one player changes the other's effort and fatigue threshold. The switch can transform an ongoing recovery into convergence toward high fatigue, or it can generate a cascade toward (B, B).

These mechanisms explain why a player can be stronger in primitives, exert more effort, and control more territory initially, yet lose both the probability advantage and the territorial majority in the long run.

6 Empirical evidence

6.1 Data, measurement, and empirical strategy

The model highlights the role of relative military recovery in determining the outcome of a confrontation. We investigate this prediction using dyadic militarized interstate disputes from the Correlates of War (COW) project, combined with country-level material-capabilities series and historical fertility estimates. Dispute histories and outcomes come from the militarized interstate dispute data (Palmer et al., 2022; Maoz et al., 2019); military personnel and other national resources are drawn from the National Material Capabilities series (Singer, 1988; Correlates of War Project, 2017); and historical total fertility rates are linked from Gapminder (Gapminder Foundation). The unit of observation is a dispute involving states A and B, with the two countries ordered consistently by their identifiers. For each dispute we retain the initial and final years, construct country-specific changes in military personnel, and merge fertility histories preceding the dispute's onset.

Our outcome Y_d equals one when state A records a victory (outcome codes 1 or 4) and zero otherwise. Thus, $Y_d = 0$ means that A does not record a victory, rather than necessarily suffering an outright defeat. Our measure of relative military recovery is

$$R_d = \mathbf{1}\{\Delta M_{A,d} > \Delta M_{B,d}\}, \qquad \Delta M_{i,d} = M_{i,T_d} - M_{i,t_d}, \tag{6.1}$$

where $M_{i,t}$ denotes military personnel and t_d and T_d denote the initial and final years of dispute d. The indicator is constructed from changes in the personnel series used in the analysis; the robustness exercise below requires both changes to be observed. Military personnel are an observable but imperfect counterpart of the model's effective fighting strength: measured changes may also reflect mobilization, demobilization, and strategic responses to the dispute itself.

To isolate variation associated with the demographic capacity to replenish personnel, we use the bilateral historical fertility differential

$$Z_d = \sum_{\ell=15}^{18} \big(F_{A,t_d-\ell} - F_{B,t_d-\ell}\big), \tag{6.2}$$

where $F_{i,t}$ is the total fertility rate of country i in year t. The 15–18-year window precedes the dispute and captures cohorts approaching military-relevant ages. This is a proxy for potential recruitment capacity rather than a direct measure of available recruits; fertility is not itself equivalent to surviving cohort size or military eligibility.

We estimate the first stage and structural equation

$$R_d = \pi Z_d + \alpha_A + \gamma_B + \lambda_{t_d} + \mu_{T_d} + u_d, \tag{6.3}$$

$$Y_d = \beta R_d + \alpha_A + \gamma_B + \lambda_{t_d} + \mu_{T_d} + \varepsilon_d. \tag{6.4}$$

The specifications include separate fixed effects for states A and B and for the dispute's starting and ending years. Standard errors are clustered by unordered country pair. We report OLS, the first stage, the reduced form, and two-stage least squares (2SLS) on the same IV estimation sample. The instrument is relevant if historical fertility differentials predict relative personnel recovery; its exclusion requires that, conditional on the included effects, these differentials influence dispute outcomes only through the recovery margin. We assess selected alternative channels below without treating those exercises as a definitive test of exclusion.

Table 3: Descriptive statistics in the baseline IV sample

Variable	N	Mean	SD	Min	Max
Main variables					
A records victory	3,454	0.120	0.325	0	1
A's personnel change exceeds B's	3,454	0.124	0.330	0	1
Historical fertility differential (15–18)	3,454	-2.139	7.806	-24.600	22.650
Change in A's military personnel	3,447	37.195	655.862	-10,000	10,322
Change in B's military personnel	3,446	24.353	460.722	-4,627	8,293
Institutional characteristics at dispute onset					
Democracy score gap (A minus B)	3,126	2.023	10.329	-20	20
Executive constraints gap	2,842	0.501	3.541	-6	6
Executive recruitment competitiveness gap	2,842	0.296	1.495	-3	3
Executive recruitment openness gap	2,842	0.281	1.845	-4	4
Political participation regulation gap	2,842	0.040	1.383	-4	4
Political participation competitiveness gap	2,842	0.336	2.158	-5	5
Same regime category	3,126	0.363	0.481	0	1
Changes in bilateral economic and institutional gaps					
Military expenditure gap	3,272	421,394.857	6,191,420.086	-4.749×10^7	1.703×10^8
Industrial production gap	3,438	131.834	2,669.247	-42,258	49,695
GDP gap	2,723	8,523.630	71,255.786	-363,676	1,628,205
Total population gap	3,447	417.168	6,638.083	-123,505	137,632
Primary energy consumption gap	3,409	3,027.091	32,817.638	-228,646	874,015
Political participation competitiveness gap	2,764	-0.007	0.266	-3	2
Same-regime indicator	3,081	0.004	0.134	-1	1

Notes: All statistics are computed among observations in the baseline IV estimation sample, with variable-specific N reflecting additional missing values. Bilateral gaps are defined as A minus B; changes in gaps are final minus initial values. The military-personnel and national-resource variables retain their source-data units.

6.2 Baseline estimates

Table 4 presents the main results. The first stage indicates that a larger historical fertility differential in favor of state A predicts a higher probability that its personnel change exceeds that of state B. The coefficient is 0.0052 (standard error 0.0015, $p < 0.01$). The reduced form is also positive: a one-unit increase in the fertility differential is associated with a 0.0048 increase in the probability that A records a victory ($p < 0.01$). The positive reduced form is consistent with the model's prediction that demographic capacity matters for the outcome of a dispute through relative military recovery.

The magnitude of the IV estimate is substantially larger than its OLS counterpart. This difference may reflect several factors. First, contemporaneous military manpower adjustments are likely to respond to the evolution of a dispute, generating simultaneity and potentially attenuating the OLS association. Second, the IV estimator isolates variation in relative manpower recovery associated with historical fertility differentials, which need not identify the same average relationship captured by OLS. In the presence of heterogeneous treatment effects, the IV estimate may therefore place greater weight on disputes in which demographic conditions are particularly consequential for military recovery. Nevertheless, the size of the IV coefficient, together with its relatively wide confidence interval, calls for caution in interpreting its magnitude. We accordingly emphasize the positive direction of the estimated relationship rather than treating the point estimate as a precisely measured average effect.

The Kleibergen–Paap rk Wald F statistic is 12.290, above the conventional benchmark of 10, and the underidentification test rejects at $p < 0.001$. These diagnostics provide evidence of instrument relevance, although an F statistic above 10 is not a guarantee against weak-instrument distortions. The baseline contains 3,454 disputes and 900 country-pair clusters.

6.3 Robustness to sample definition and initial institutions

We next examine whether the baseline result depends on how the personnel-change indicator is observed. The baseline construction codes the relative-recovery indicator as zero when the comparison of personnel changes cannot be established. Restricting the sample to disputes with observed personnel changes for both countries yields a closely similar IV estimate of 0.9470 (standard error 0.3949). The first-stage statistic remains above 10 (12.183), suggesting that missing personnel-change observations are not driving the main estimate. This comparison is especially relevant because the underlying military-personnel series is incomplete for some dispute-years.

A second concern is that initial political institutions may be related to both mobilization

Table 4: Historical fertility, relative military recovery, and dispute outcomes

	First stage	Reduced form	OLS	2SLS
Historical fertility differential	0.0052***	0.0048***		
	(0.0015)	(0.0014)		
Relative military recovery			0.0603***	0.9158**
			(0.0225)	(0.3930)
Observations	3,454	3,454	3,454	3,454
Country-pair clusters	900	900	900	900
Kleibergen–Paap rk Wald F				12.290
Country and start/end-year FE	Yes	Yes	Yes	Yes

Notes: The dependent variables are relative military recovery in the first stage and a recorded victory for state A in the remaining columns. The excluded instrument is the historical fertility differential. Country-pair clustered standard errors in parentheses. $^{*}p < 0.10$, $^{**}p < 0.05$, $^{***}p < 0.01$.

capacity and conflict outcomes. We therefore add two predetermined characteristics in separate IV specifications: the difference in democracy scores at the start of the dispute and an indicator that the two countries initially belong to the same regime category. Both controls are measured at onset, rather than as changes during the dispute, to avoid conditioning on institutional responses that could be affected by the conflict. The IV coefficient is 1.0053 with the initial democracy gap and 1.0072 with common regime status; both estimates remain significant at the five-percent level. Their respective Kleibergen–Paap statistics are 10.891 and 10.629. Because institutional data are not available for every dispute, these specifications use 3,120 observations rather than the full baseline sample.

Table 5 brings the sample and institutional robustness exercises together. The estimates remain positive and statistically significant across specifications, although differences in estimation samples should be considered when comparing their magnitudes.

6.4 Selected alternative-channel diagnostics

The exclusion restriction would be threatened if historical fertility differentials also predicted conflict outcomes through other bilateral developments. We investigate a set of observable economic channels by regressing changes in the bilateral gaps in military expenditure, industrial production, GDP, total population, and primary energy consumption on the historical fertility differential, absorbing the same country and year effects and clustering at the country-pair level. These outcomes capture several aspects of economic and material capacity that could plausibly affect dispute outcomes independently of personnel recovery.

Table 6 reports the results alongside two institutional diagnostics: changes in political participation competitiveness and changes in whether the countries share the same regime

Table 5: IV robustness: observed personnel changes and initial institutions

	Baseline	Observed changes	Initial democracy gap	Same initial regime
Relative military recovery	0.9158**	0.9470**	1.0053**	1.0072**
	(0.3930)	(0.3949)	(0.4251)	(0.4255)
Democracy score gap at onset			-0.0007	
			(0.0013)	
Same regime category at onset				-0.0181
				(0.0204)
Observations	3,454	3,439	3,120	3,120
Country-pair clusters	900	893	794	794
Kleibergen–Paap rk Wald F	12.290	12.183	10.891	10.629
Country and start/end-year FE	Yes	Yes	Yes	Yes

Notes: Each column estimates a separate 2SLS model instrumenting relative military recovery with the historical fertility differential. The observed-changes column excludes disputes with missing changes in either country's personnel. Institutional variables refer to dispute onset. Standard errors are clustered by country pair. $^{*}p < 0.10$, $^{**}p < 0.05$, $^{***}p < 0.01$.

category. None of these seven selected associations is statistically distinguishable from zero at the ten-percent level. The estimates provide a useful check against these particular observable pathways; they do not imply that the fertility instrument is unrelated to all possible demographic, economic, or political changes. In particular, these exercises should be interpreted as diagnostics rather than as a formal validation of the exclusion restriction.

Table 6: Historical fertility and selected alternative channels

	Military spending	Industrial production	GDP	Total population	Energy use	Participation competition	Same regime
Historical fertility differential	-3462.5397	-29.8816	-211.2979	-12.3058	-81.4936	0.0012	-0.0003
	(37883.4381)	(19.8441)	(334.2008)	(36.9285)	(134.7660)	(0.0018)	(0.0006)
Observations	3,253	3,438	2,690	3,447	3,408	2,745	3,075
Country-pair clusters	856	890	706	894	868	712	784
Country and start/end-year FE	Yes	Yes	Yes	Yes	Yes	Yes	Yes

Notes: Each column reports a separate reduced-form regression of a change in the indicated bilateral gap on the historical fertility differential. The last column concerns the change in an indicator that both countries belong to the same regime category. Standard errors are clustered by country pair. These are selected, theoretically motivated channel diagnostics, not an exhaustive set of specification searches.

6.5 Multiyear disputes and the measurement of recovery

Military-personnel and fertility data are observed annually, limiting our ability to measure replenishment within disputes that begin and end in the same calendar year. For such disputes, the measured change in military personnel is mechanically zero whenever both annual endpoints are observed. This limitation is arguably less consequential for short confrontations, in which substantial replenishment may be less likely to occur. Nevertheless, we examine multiyear disputes separately to assess whether the positive association between

relative military recovery and victory is driven by the mechanically zero changes in shorter disputes.

Table 7 reports two complementary OLS associations within multiyear disputes. Column (1) shows that state A is 10.7 percentage points more likely to record a victory when it begins with fewer military personnel than state B; this estimate is significant at the ten-percent level. Column (2) shows that a greater observed increase in A's military personnel relative to B's is associated with a 9.3 percentage-point higher probability of victory. The second specification excludes disputes with missing personnel changes for either country. These patterns are consistent with the possibility that initial military disadvantage can be overcome and that relative recovery matters in longer confrontations. Importantly, the positive recovery–victory association is present even after excluding within-year disputes.

Table 7: Initial military disadvantage and relative recovery in multiyear disputes

	(1) A wins	(2) A wins
A initially weaker	0.1073*	
	(0.0602)	
Relative military recovery		0.0932***
		(0.0321)
Observations	749	797
Country-pair clusters	317	341
Country and start/end-year FE	Yes	Yes

Notes: Both columns restrict the sample to disputes spanning more than one calendar year. The dependent variable equals one when state A records a victory. In column (1), A is initially weaker if its military personnel at dispute onset are lower than B's; ties and missing initial personnel are excluded. In column (2), relative military recovery equals one if A's change in military personnel exceeds B's; observations with missing personnel changes are excluded. Both specifications include state-A, state-B, start-year, and end-year fixed effects. Country-pair clustered standard errors in parentheses. $^{*}p < 0.10$, $^{**}p < 0.05$, $^{***}p < 0.01$.

6.6 Interpretation

Taken together, the results offer empirical support for the recovery margin emphasized by the model. Fertility differentials measured well before a dispute predict relative changes in military personnel, and the same differentials are positively associated with a recorded victory. The IV estimate remains positive when personnel changes must be directly observed and when controlling for two distinct dimensions of the disputants' initial political institutions. Selected economic and institutional diagnostics do not reveal systematic associations with several competing pathways. The evidence therefore points to relative military recovery as a

potentially important determinant of dispute outcomes, while the interpretation of the 2SLS coefficient as causal remains conditional on the instrument's exclusion restriction and the limitations of observed personnel changes as a measure of effective military strength.

Discussion and concluding remarks

Military superiority is not necessarily a persistent advantage. In prolonged confrontations, the capacity to sustain military effort and recover from accumulated fatigue may be as important as the resources available at the outset. This paper develops a dynamic contest framework in which military effort affects both the probability of success and the evolution of fatigue, generating endogenous recovery thresholds, multiple long-run regimes, and the possibility of strategic reversals.

The central insight is that greater military strength can become dynamically self-defeating. Players that are less vulnerable to fatigue exert greater effort and initially enjoy a strategic advantage. However, higher effort also reduces their capacity to recover, potentially trapping them in a persistent high-fatigue regime. Conversely, a more fatigue-vulnerable player may optimally exercise restraint, remain within the recovery region, and eventually overturn the initial balance of power. In the separable exponential contest, we establish this mechanism through a globally verified Markov-perfect equilibrium, showing that strategic reversal can occur even before the recovering player has fully eliminated its fatigue stock.

Introducing state dependence extends the mechanism from contest success to territorial control. When territory affects the marginal returns to military effort, a transition between fatigue regimes changes not only the recovering player's incentives but also those of its opponent. Consequently, recovery can shift the long-run territorial balance, alter the opponent's fatigue threshold, and generate switching cascades. The resulting dynamics highlight how temporary differences in recovery capacity can produce persistent changes in the strategic configuration of a conflict. These territorial transitions are characterized within a piecewise-stationary framework, providing a tractable description of regime-dependent adjustment.

The empirical analysis offers complementary evidence for the relevance of the proposed mechanism. Combining historical militarized interstate disputes with military-personnel and fertility data, we find that relative military manpower recovery is positively associated with dispute success. Instrumenting relative recovery with historical fertility differentials yields a positive and statistically significant estimate, substantially larger than its OLS counterpart. The results are consistent with the view that demographic conditions affecting military replenishment can influence the evolution of confrontations, although their causal interpretation depends on the identifying assumptions underlying the instrumental-variable

strategy.

More broadly, the analysis suggests that the outcome of a military confrontation cannot be understood solely through initial capabilities or contemporaneous effort. The interaction between military mobilization, accumulated fatigue, and replenishment creates a dynamic dimension of strategic advantage in which restraint may improve long-run prospects and apparent superiority may prove unsustainable.

References

Vera Angelova, Thomas Giebe, and Radosveta Ivanova-Stenzel. Competition and fatigue. *Journal of Economic Behavior & Organization*, 198:236–249, 2022. doi: 10.1016/j.jebo.2022.03.032.

Carmen Beviá and Luis C. Corchón. Endogenous strength in conflicts. *International Journal of Industrial Organization*, 31(3):297–306, 2013. doi: 10.1016/j.ijindorg.2012.09.002.

Correlates of War Project. National material capabilities data, version 5.0: Documentation. University of North Texas, February 1, 2017. URL `https://correlatesofwar.org/data-sets/national-material-capabilities/`. Version 5.0 documentation supplied with the research data; coverage 1816–2012.

Serhat Doğan, Kerim Keskin, and Çağrı Sağlam. Analyzing strategic behavior in a dynamic model of bargaining and war. *Journal of Economics*, 140(3):233–257, 2023. doi: 10.1007/s00712-023-00838-7.

James D. Fearon. Rationalist explanations for war. *International Organization*, 49(3):379–414, 1995. doi: 10.1017/S0020818300033324.

Gapminder Foundation. Babies per woman (total fertility rate): Data and documentation. Gapminder data series. URL `https://www.gapminder.org/data/documentation/gd008/`. Historical estimates and modern demographic series; accessed November 2026.

Michelle R. Garfinkel and Stergios Skaperdas. Economics of conflict: An overview. In Todd Sandler and Keith Hartley, editors, *Handbook of Defense Economics*, volume 2, pages 649–709. Elsevier, 2007. doi: 10.1016/S1574-0013(06)02022-9.

Jack Hirshleifer. Conflict and rent-seeking success functions: Ratio vs. difference models of relative success. *Public Choice*, 63(2):101–112, 1989.

Kerim Keskin and Çağrı Sağlam. Fatigue accumulation in dynamic contests. *Operations Research Letters*, 50(3):268–273, 2022. doi: 10.1016/j.orl.2022.02.009.

Zeev Maoz, Paul L. Johnson, Jasper Kaplan, Fiona Ogunkoya, and Aaron Shreve. The dyadic militarized interstate disputes (MIDs) dataset version 3.0: Logic, characteristics, and comparisons to alternative datasets. *Journal of Conflict Resolution*, 2019. doi: 10.1177/0022002718784158.

Glenn Palmer, Roseanne W. McManus, Vito D'Orazio, Michael R. Kenwick, Mikaela Karstens, Chase Bloch, Nick Dietrich, Kayla Kahn, Kellan Ritter, and Michael J. Soules. The mid5 dataset, 2011–2014: Procedures, coding rules, and description. *Conflict Management and Peace Science*, 39(4):470–482, 2022. doi: 10.1177/0738894221995743. Article of record for COW MID version 5.0; online publication 2021.

Robert Powell. Bargaining and learning while fighting. *American Journal of Political Science*, 48(2):344–361, 2004. doi: 10.1111/j.0092-5853.2004.00074.x.

J. David Singer. Reconstructing the correlates of war dataset on material capabilities of states, 1816–1985. *International Interactions*, 14:115–132, 1988.

A Proofs for the state-independent exponential contest

Player i's current-value Hamiltonian is

$$\mathcal{H}_i = \pi \frac{1 + \mathrm{e}^{-g_j} - \mathrm{e}^{-g_i}}{2} - g_i - \rho_i c_i^2 + \lambda_i (g_i + c_i - c_i^2 - k). \tag{A.1}$$

The effort first-order condition is

$$\frac{\pi}{2} \mathrm{e}^{-g_i} = 1 - \lambda_i. \tag{A.2}$$

The current-value costate equation is

$$\begin{aligned} \dot{\lambda}_i &= r\lambda_i - \frac{\partial \mathcal{H}_i}{\partial c_i} \\ &= (r - 1 + 2c_i)\lambda_i + 2\rho_i c_i. \end{aligned} \tag{A.3}$$

With $r = 1$, an interior stationary point $c_i > 0$ satisfies

$$0 = 2c_i(\lambda_i + \rho_i),$$

and hence $\lambda_i = -\rho_i$. At the boundary we impose $\lambda_i = 0$.

Proof of Proposition 1. Substituting λ_i^R into (A.2) gives

$$\mathrm{e}^{-g_i^R} = \frac{2a_i^R}{\pi}.$$

Taking logarithms yields (3.2). Substitution into

$$p_i^R = \frac{1}{2} + \frac{\mathrm{e}^{-g_j^R} - \mathrm{e}^{-g_i^R}}{2}$$

gives

$$p_i^R = \frac{1}{2} + \frac{a_j^R - a_i^R}{\pi}.$$

Equations (3.4)–(3.7) follow by assigning the regime-specific wedges. □

A.1 Fatigue dynamics

Equation (3.10) can be written as

$$\dot{c} = -\left(c - c^-(g)\right)\left(c - c^+(g)\right) = \left(c - c^-(g)\right)\left(c^+(g) - c\right). \tag{A.4}$$

Proof of Proposition 2. The discriminant of the stationary quadratic is $\Delta(g) = 1 + 4(g - k)$.

If $k < g$, then $\Delta > 1$, $c^- < 0 < c^+$, and the vector field is positive below c^+ and negative above it. This proves part (i).

If $k = g$, then $\dot{c} = c(1 - c)$, proving part (ii).

If $g < k < g + 1/4$, then $0 < \Delta < 1$, so

$$0 < c^- < \frac{1}{2} < c^+ < 1.$$

The sign pattern of (A.4) is negative on $(0, c^-)$, positive on (c^-, c^+), and negative on (c^+, ∞). Projection makes zero absorbing, proving part (iii).

If $k = g + 1/4$, then

$$\dot{c} = -\left(c - \frac{1}{2}\right)^2,$$

which proves part (iv). If $k > g + 1/4$, the quadratic has no real roots and is strictly negative, proving part (v).

For the transition path, separate variables in (A.4):

$$\frac{\mathrm{d}c}{(c - c^-)(c^+ - c)} = \mathrm{d}t.$$

Since

$$\frac{1}{(c-c^-)(c^+-c)} = \frac{1}{c^+-c^-}\left[\frac{1}{c-c^-} + \frac{1}{c^+-c}\right],$$

integration yields

$$\frac{c(t)-c^-}{c^+-c(t)} = \frac{c(0)-c^-}{c^+-c(0)}\mathrm{e}^{(c^+-c^-)t}.$$

Because $c^+ - c^- = \sqrt{\Delta(g)}$, solving for $c(t)$ gives (3.16). Setting $c(T_0) = 0$ gives (3.17). □

A.2 Canonical stability

The interior control from (A.2) is

$$g_i(\lambda_i) = \ln\left[\frac{\pi}{2(1-\lambda_i)}\right], \qquad \frac{\partial g_i}{\partial \lambda_i} = \frac{1}{1-\lambda_i}. \tag{A.5}$$

The canonical subsystem at $r = 1$ is

$$\dot{c}_i = g_i(\lambda_i) + c_i - c_i^2 - k, \tag{A.6}$$

$$\dot{\lambda}_i = 2c_i(\lambda_i + \rho_i). \tag{A.7}$$

Proof of Proposition 3. At $\lambda_i = -\rho_i$, the Jacobian is

$$J(c_i^*) = \begin{pmatrix} 1 - 2c_i^* & \dfrac{1}{1+\rho_i} \\ 0 & 2c_i^* \end{pmatrix}.$$

Its eigenvalues are $1 - 2c_i^*$ and $2c_i^*$. At c_i^-, both are positive. At c_i^+, the first is negative and the second positive. Hence the lower point is a source and the upper point is a saddle. □

A.3 Coexistence, comparative statics, and reversal

Proof of Proposition 4. The boundary is viable if and only if

$$g_i^{\mathrm{B}} - k \le 0,$$

which is $g_i^{\mathrm{B}} \le k$. A positive high-fatigue root exists if and only if

$$1 + 4(g_i^{\mathrm{I}} - k) > 0,$$

or $k < g_i^{\mathrm{I}} + 1/4$. Combining the two gives (3.19). Since

$$g_i^{\mathrm{B}} - g_i^{\mathrm{I}} = \ln(1+\rho_i),$$

the interval is nonempty if and only if (3.20) holds. In the separable exponential contest, each player's effort depends only on its own regime, so (3.21) supports every regime profile. □

Proof of Proposition 5. Differentiate

$$g_i^{\mathrm{I}} = \ln\left(\frac{\pi}{2}\right) - \ln(1+\rho_i)$$

to obtain (3.22). Since

$$\frac{\partial c^-}{\partial g} = -\frac{1}{\sqrt{1+4(g-k)}}, \qquad \frac{\partial c^+}{\partial g} = \frac{1}{\sqrt{1+4(g-k)}},$$

the chain rule gives (3.23) and (3.24). □

A.4 Global verification of the state-independent dynamic game

The proofs below do not assume that stationary regime efforts remain optimal along transitions. They derive the policy from the discounted control problem with the *projected* fatigue law.

Lemma 1 (An exact discounted payoff identity)**.** *For one player, write the projected dynamics in regulated form:*

$$\dot{c} = g + c - c^2 - k + L, \qquad L = \mathbf{1}_{\{c=0\}}(k-g)_+ \geq 0. \tag{A.8}$$

For a nonnegative measurable control with $\int_0^\infty \mathrm{e}^{-t}(g(t)+c(t)^2)\,\mathrm{d}t < \infty$*,*

$$\int_0^\infty \mathrm{e}^{-t}c(t)^2\,\mathrm{d}t = c(0) + \int_0^\infty \mathrm{e}^{-t}\big[g(t) - k + L(t)\big]\,\mathrm{d}t. \tag{A.9}$$

Consequently the reduced objective (3.25) *becomes*

$$J^{\mathrm{own}}(c_0, g) = -\rho c_0 + \int_0^\infty \mathrm{e}^{-t}\big[f(g) - \rho g + \rho k - \rho L\big]\,\mathrm{d}t. \tag{A.10}$$

Proof. Because $\frac{\mathrm{d}}{\mathrm{d}t}(\mathrm{e}^{-t}c) = \mathrm{e}^{-t}(g - c^2 - k + L)$, integration on $[0,T]$ gives

$$\int_0^T \mathrm{e}^{-t}c(t)^2\,\mathrm{d}t = c_0 + \int_0^T \mathrm{e}^{-t}(g-k+L)\,\mathrm{d}t - \mathrm{e}^{-T}c(T).$$

To justify the terminal limit directly, note that $c - c^2 \le 1/4$ in the interior, whereas at $c = 0$ the projected velocity is $\max\{g - k, 0\} \le g$. Consequently, every admissible trajectory satisfies

$$0 \le c(T) \le c_0 + \frac{T}{4} + \int_0^T g(t)\,\mathrm{d}t.$$

Set $h(t) = \mathrm{e}^{-t} g(t)$, which belongs to $L^1([0,\infty))$ by admissibility. Splitting the discounted effort integral at $T/2$ gives

$$\mathrm{e}^{-T} \int_0^T g(t)\,\mathrm{d}t \le \mathrm{e}^{-T/2} \int_0^\infty h(t)\,\mathrm{d}t + \int_{T/2}^\infty h(t)\,\mathrm{d}t \longrightarrow 0.$$

It follows that $\mathrm{e}^{-T} c(T) \to 0$. The discounted identity then follows by letting $T \to \infty$ in the finite-horizon equality. Substituting this identity into $J^{\mathrm{own}} = \int_0^\infty \mathrm{e}^{-t}[f(g) - \rho c^2]dt$ yields (A.10); in particular, $f(g)$ already contains the direct effort cost $-g$, so the additional term is $-\rho g$, not $-(1+\rho)g$. □

Lemma 2 (Global bound and the high-fatigue branch)**.** *Under Assumption 2, every admissible control satisfies*

$$J^{\mathrm{own}}(c_0, g) \le A - \rho c_0, \quad A = f(g^{\mathrm{I}}) - \rho g^{\mathrm{I}} + \rho k. \tag{A.11}$$

For $c_0 \ge c^-(g^{\mathrm{I}})$, this bound is attained by $g(t) = g^{\mathrm{I}}$ for all $t \ge 0$; hence $V(c_0) = A - \rho c_0$ on the entire high-fatigue region.

Proof. Strict concavity of $f(g) - (\rho g)$ implies

$$\max_{g \ge 0}\{f(g) - \rho g\} = f(g^{\mathrm{I}}) - \rho g^{\mathrm{I}}, \qquad g^{\mathrm{I}} = \ln \frac{q}{1+\rho} > 0.$$

Since $L \ge 0$, the transformed payoff (A.10) yields the global bound. At $c_0 \ge c^-$, holding effort at g^{I} keeps fatigue strictly positive at every finite time and the trajectory converges to c^+ (or stays at c^- when initialized there). Hence $L = 0$ almost everywhere and the bound is attained. □

Lemma 3 (Regular backward recovery characteristic)**.** *Under Assumption 2, the solution of* (3.29)–(3.30) *obeys*

$$0 < C(s) < c^-, \quad -\rho < \Lambda(s) < 0, \quad C'(s) > 0, \quad \Lambda'(s) < 0 \qquad (s > 0), \tag{A.12}$$

and

$$\lim_{s \to \infty} (C(s), \Lambda(s)) = (c^-, -\rho). \tag{A.13}$$

In particular the costate is a single-valued smooth function $\ell(c) = \Lambda(C^{-1}(c))$ on $(0, c^-)$, with

$$\ell(0) = 0, \quad \ell(c^-) = -\rho, \qquad \ell'(c) = \frac{2c(\ell(c) + \rho)}{G(\ell(c)) + c - c^2 - k} < 0. \tag{A.14}$$

Proof. Set $z := \Lambda + \rho$, so $z(0) = \rho > 0$ and $z' = -2Cz$. Define the backward velocity $h := k - G(\Lambda) - C + C^2 = C'$. At the origin, $h(0) = k - g^{\mathrm{B}} > 0$. Along the characteristic,

$$\frac{\mathrm{d}h}{\mathrm{d}s} = (2C - 1)h + \frac{2Cz}{1 - \Lambda}. \tag{A.15}$$

Whenever $C > 0, z > 0$ and $h = 0$, the derivative on the right is strictly positive. Hence h cannot cross from positive to negative for the first time; it stays positive. Since $z' = -2Cz$, one has $0 < z \leq \rho$ and $-\rho \leq \Lambda \leq 0$. Moreover, at $C = c^-$ with $z > 0$,

$$h = k - G(\Lambda) - c^- + (c^-)^2 = g^{\mathrm{I}} - G(\Lambda) < 0,$$

contradicting positivity. Therefore $C(s) < c^-$ for finite s. The increasing function C has a limit $L \in (0, c^-]$. Because $C(s)$ is eventually bounded below by a positive constant, $z(s) \to 0$. Thus $\Lambda(s) \to -\rho$. The limiting relation $h \to k - g^{\mathrm{I}} - L + L^2$ and convergence of the bounded, monotone C force $h \to 0$. Therefore L is a root of the quadratic $k - g^{\mathrm{I}} - L + L^2 = 0$. As $L \leq c^-$, we obtain $L = c^-$. Dividing the forward costate equation by the forward state equation along this characteristic gives (A.14); its negative denominator is the opposite of $h > 0$. □

Proof of Proposition 6. At $c = 0$, $g^{\mathrm{B}} = \ln q < k$ keeps the projected state at zero. Since f is strictly concave and maximized at g^{B}, $V(0) = B = f(g^{\mathrm{B}})$ and the right derivative of the candidate value at zero is $\ell(0) = 0$.

For $0 < c < c^-$ define $V_L(c) = B + \int_0^c \ell(u)\,\mathrm{d}u$. The Hamiltonian $f(g) - \rho c^2 + V_L'(c)(g + c - c^2 - k)$ is strictly concave in g, with unique maximizer $g = G(\ell(c)) > 0$. Consider its HJB residual

$$R(c) := f(G(\ell(c))) - \rho c^2 + \ell(c)\big[G(\ell(c)) + c - c^2 - k\big] - V_L(c).$$

The envelope condition $f'(G(\ell)) + \ell = 0$ and (A.14) imply

$$R'(c) = \ell'(c)\big[G(\ell(c)) + c - c^2 - k\big] - 2c(\ell(c) + \rho) = 0.$$

Since $R(0) = f(g^{\mathrm{B}}) - B = 0$, the candidate solves HJB in the recovery region.

At the threshold, $\ell(c) \to -\rho$ and $G(\ell(c)) \to g^{\mathrm{I}}$, while the state drift tends to zero. The

HJB identity therefore yields

$$\lim_{c\uparrow c^-} V_L(c) = f(g^{\mathrm{I}}) - \rho(c^-)^2 = A - \rho c^-,$$

where the last equality uses $g^{\mathrm{I}} + c^- - (c^-)^2 - k = 0$. Hence the recovery branch joins continuously to $V_H(c) = A - \rho c$ at c^-; their slopes both tend to $-\rho$. The piecewise function (3.33) is thus C^1, and HJB holds also on the high branch by direct substitution. At the boundary, its slope is zero, and the projected HJB becomes $V(0) = \max_{g\geq 0} f(g) = B$.

For any admissible control, the HJB inequality integrated along the projected state gives $V(c_0) \geq J^{\mathrm{own}}(c_0, g)$ after the terminal term $\mathrm{e}^{-T}V(c(T))$ vanishes. This term vanishes because $|V(c)| \leq C(1+c)$ and Lemma 1 establishes $\mathrm{e}^{-T}c(T) \to 0$. The feedback in (3.34) attains the HJB maximum everywhere, including at $c = 0$, and its paths have finite discounted costs; therefore equality holds and the candidate is the *global* value function. Its strict Hamiltonian concavity makes the maximizing feedback unique wherever the first-order condition is interior.

In the recovery region, the forward drift is $G(\ell(c)) + c - c^2 - k = -C'(C^{-1}(c)) < 0$. Every initial $c_0 < c^-$ corresponds to a finite backward time $C^{-1}(c_0)$, so recovery is completed in finite forward time. The feedback rises strictly as c falls. For $c > c^-$ the global bound in Lemma 2 is attained by the constant g^{I} and the state converges to c^+.

Finally, for the full contest,

$$\pi p_i - g_i - \rho_i c_i^2 = q\mathrm{e}^{-g_j} + [f(g_i) - \rho_i c_i^2].$$

The first term is independent of player i's action and own state. As each player controls only its own fatigue law, the verified policy is optimal against *any* opponent action. Hence the product feedback profile is a Markov-perfect Nash equilibrium and its induced paths are open-loop Nash equilibria. □

Proof of Proposition 7. For $0 < \rho_i < \rho_j$, the stationary efforts satisfy $g_j^{\mathrm{I}} < g_i^{\mathrm{I}} < g^{\mathrm{B}}$. By Lemma 3, the feedback of player j is continuous and strictly decreasing in fatigue from g^{B} at 0 to g_j^{I} at c_j^-. The intermediate-value theorem therefore gives a unique $c_{j,\times} \in (0, c_j^-)$ such that $g_j^*(c_{j,\times}) = g_i^{\mathrm{I}}$, equivalently $\ell_j(c_{j,\times}) = -\rho_i$. If $c_{j,\times} < c_j(0) < c_j^-$, player j follows the optimal strictly decreasing fatigue path and crosses $c_{j,\times}$ once, before reaching zero. Meanwhile i stays in the high basin with $g_i(t) = g_i^{\mathrm{I}}$. The identity

$$p_i - \frac{1}{2} = \frac{1}{2}\big(\mathrm{e}^{-g_j} - \mathrm{e}^{-g_i^{\mathrm{I}}}\big)$$

changes sign precisely when g_j rises through g_i^{I}. Integration of the strictly negative fatigue

drift proves (3.39) and the strict inequality $t_\times < T_j$. The terminal regime has $g_j = g^{\mathrm{B}}$ and $g_i = g_i^{\mathrm{I}}$, giving (3.40). All assumptions and strict initial-state inequalities persist under small perturbations, so the reversal occurs on an open, nonempty parameter/state region. □

Proof of Corollary 1. At the limiting profile (I, B),

$$W_i = \frac{\pi}{2} - \rho_i - g_i^{\mathrm{I}} - \rho_i (c_i^+)^2,$$
$$W_j = \frac{\pi}{2} + \rho_i - g^{\mathrm{B}}.$$

Consequently, $W_j - W_i = 2\rho_i - (g^{\mathrm{B}} - g_i^{\mathrm{I}}) + \rho_i (c_i^+)^2$. The identity $g^{\mathrm{B}} - g_i^{\mathrm{I}} = \ln(1+\rho_i)$ and the inequality $\ln(1+\rho_i) < \rho_i$ establish the result. □

B Proofs for the state-dependent exponential contest

B.1 Hamiltonians and stationary first-order conditions

Write $x = x_i$. Player i's current-value Hamiltonian is

$$\mathcal{H}_i = \pi p_i - g_i - \rho_i c_i^2 + \lambda_i (g_i + c_i - c_i^2 - k) + \mu_i (p_i - x), \tag{B.1}$$

where

$$p_i = \frac{1 + x\mathrm{e}^{-g_j} - (1-x)\mathrm{e}^{-g_i}}{2}.$$

The effort condition is

$$(1-x)\frac{\mathrm{e}^{-g_i}}{2}(\pi + \mu_i) = 1 - \lambda_i. \tag{B.2}$$

The costate equations are

$$\dot{\lambda}_i = (r - 1 + 2c_i)\lambda_i + 2\rho_i c_i, \tag{B.3}$$

$$\dot{\mu}_i = (r+1)\mu_i - \frac{\mathrm{e}^{-g_i} + \mathrm{e}^{-g_j}}{2}(\pi + \mu_i). \tag{B.4}$$

Player j's Hamiltonian, using the same territorial state x, is

$$\mathcal{H}_j = \pi(1 - p_i) - g_j - \rho_j c_j^2 + \lambda_j (g_j + c_j - c_j^2 - k) + \mu_j (p_i - x). \tag{B.5}$$

Its effort condition is

$$x\frac{\mathrm{e}^{-g_j}}{2}(\pi - \mu_j) = 1 - \lambda_j, \tag{B.6}$$

and its territorial costate satisfies

$$\dot{\mu}_j = (r+1)\mu_j - \frac{\mathrm{e}^{-g_i} + \mathrm{e}^{-g_j}}{2}(\mu_j - \pi). \tag{B.7}$$

At $r = 1$, stationarity implies

$$\mu_i = \frac{\pi(y_i + y_j)}{2 - y_i - y_j}, \tag{B.8}$$

$$\mu_j = -\frac{\pi(y_i + y_j)}{2 - y_i - y_j}. \tag{B.9}$$

Consequently,

$$\pi + \mu_i = \pi - \mu_j = \frac{2\pi}{2 - y_i - y_j}. \tag{B.10}$$

Proof of Proposition 8. Using $a_i^R = 1 - \lambda_i^R$, equations (B.2)–(B.10) give

$$2\pi(1-x)y_i = a_i^R(2 - y_i - y_j), \tag{B.11}$$

$$2\pi x y_j = a_j^R(2 - y_i - y_j). \tag{B.12}$$

Dividing (B.12) by (B.11) yields

$$y_j = \frac{a_j^R}{a_i^R}\frac{1-x}{x}y_i. \tag{B.13}$$

Substituting into (B.11) and solving gives

$$y_i = \frac{2x a_i^R}{2\pi x(1-x) + (1-x)a_j^R + x a_i^R}.$$

Equation (B.13) gives the expression for y_j. Since

$$g_i = -\ln(2y_i),$$

equations (4.8) and (4.9) follow.

The territorial stationary condition is

$$x = \frac{1}{2} + x y_j - (1-x)y_i.$$

Substitution of (4.6)–(4.7) gives

$$x = \frac{1}{2} + \frac{2x(1-x)(a_j^R - a_i^R)}{D_R(x)}. \tag{B.14}$$

Multiplying through by $D_R(x)$ and collecting powers of x yields (4.10). □

B.2 Uniqueness of the economic root

Proof of Proposition 9. Continuity of the right-hand side of (B.14) implies existence because the fixed-point residual is positive at $x = 0$ and negative at $x = 1$.

If $a_j^R = a_i^R$, equation (B.14) gives $x = 1/2$.

Suppose $a_j^R > a_i^R$. Any fixed point must satisfy $x > 1/2$. Define

$$B := a_j^R, \qquad A := a_i^R, \qquad \delta := \frac{B - A}{B} \in (0, 1), \qquad \tau := \frac{2\pi}{B}.$$

Rearranging (B.14) gives

$$\delta = \Psi_\tau(x) := \frac{(2x - 1)\left[1 + \tau x(1 - x)\right]}{x(3 - 2x)}, \qquad x \in \left(\frac{1}{2}, 1\right). \tag{B.15}$$

We have $\Psi_\tau(1/2) = 0$ and $\Psi_\tau(1) = 1$. Its derivative is

$$\Psi'_\tau(x) = \frac{4x^2 - 4x + 3 + \tau x^2(4x^2 - 12x + 7)}{x^2(3 - 2x)^2}. \tag{B.16}$$

If $4x^2 - 12x + 7 \geq 0$, the numerator is strictly positive. If $4x^2 - 12x + 7 < 0$, the condition $\Psi_\tau(x) < 1$ implies

$$\tau < \frac{2x + 1}{x(2x - 1)}.$$

Because the coefficient on τ in (B.16) is then negative, the derivative numerator is bounded below by its value at the upper bound:

$$\frac{(x - 1)(2x - 3)(4x^2 + 4x - 1)}{2x - 1} > 0$$

for $x \in (1/2, 1)$. Hence Ψ_τ is strictly increasing wherever it takes values in $(0, 1)$, and the solution to (B.15) is unique.

If $a_j^R < a_i^R$, exchange the player labels and use the symmetry

$$x^*(A, B) = 1 - x^*(B, A).$$

This proves uniqueness and (4.14). □

B.3 Cardano representation

Write the cubic as

$$ax^3 + bx^2 + cx + d = 0, \tag{B.17}$$

where

$$\begin{aligned} a &= 4\pi, \\ b &= -2\left(3\pi + a_j^R - a_i^R\right), \\ c &= 2\pi + a_j^R - 3a_i^R, \\ d &= a_j^R. \end{aligned} \tag{B.18}$$

Define

$$P = \frac{3ac - b^2}{3a^2}, \tag{B.19}$$

$$Q = \frac{27a^2d - 9abc + 2b^3}{27a^3}, \tag{B.20}$$

$$\Delta_C = \left(\frac{Q}{2}\right)^2 + \left(\frac{P}{3}\right)^3. \tag{B.21}$$

Let

$$C = \sqrt[3]{-\frac{Q}{2} + \sqrt{\Delta_C}}, \qquad D = \sqrt[3]{-\frac{Q}{2} - \sqrt{\Delta_C}},$$

and

$$\omega = \frac{-1 + \mathrm{i}\sqrt{3}}{2}, \qquad \omega^2 = \frac{-1 - \mathrm{i}\sqrt{3}}{2}.$$

The three algebraic roots are

$$x_1 = -\frac{b}{3a} + C + D, \tag{B.22}$$

$$x_2 = -\frac{b}{3a} + \omega C + \omega^2 D, \tag{B.23}$$

$$x_3 = -\frac{b}{3a} + \omega^2 C + \omega D. \tag{B.24}$$

Proposition 9 identifies the unique root in $(0, 1)$. In the interior–interior case,

$$-\frac{b}{3a} = \frac{1}{2} - \frac{\rho_i - \rho_j}{6\pi},$$

recovering the representation in the underlying calculations.

B.4 Territorial transition and regime consistency

Proof of Proposition 10. With constant efforts,

$$p_i = \frac{1 - \mathrm{e}^{-g_i^R}}{2} + x_i \frac{\mathrm{e}^{-g_i^R} + \mathrm{e}^{-g_j^R}}{2}.$$

Therefore

$$\dot{x}_i = \frac{1 - 2y_i^R}{2} - (1 - y_i^R - y_j^R)x_i.$$

Positive efforts imply $0 < y_i^R, y_j^R < 1/2$, so $\gamma_R = 1 - y_i^R - y_j^R > 0$. Solving the linear equation gives (4.21) and (4.22). □

Proof of Proposition 11. If $R_i = \mathrm{B}$, projected boundary viability requires $g_i^R - k \leq 0$, yielding (4.24). If $R_i = \mathrm{I}$, a real high-fatigue root requires

$$1 + 4(g_i^R - k) > 0,$$

which is (4.25). Applying these conditions to every occurrence of a boundary or interior player across the four regime profiles gives (4.26). □

Proof of Proposition 12. In regime (I, I), the wedges are

$$a_i^{\mathrm{II}} = 1 + \rho_i, \qquad a_j^{\mathrm{II}} = 1 + \rho_j.$$

If $\rho_i < \rho_j$, then $a_i^{\mathrm{II}} < a_j^{\mathrm{II}}$, and Proposition 9 implies $x_{\mathrm{II}}^* > 1/2$.

In regime (I, B),

$$a_i^{\mathrm{IB}} = 1 + \rho_i > 1 = a_j^{\mathrm{IB}}.$$

Proposition 9 therefore implies $x_{\mathrm{IB}}^* < 1/2$. □

Proof of Proposition 13. After player j reaches the boundary, stationary-regime adjustment replaces the (I, I) effort pair by the (I, B) pair. Player i's fatigue law becomes

$$\dot{c}_i = g_i^{\mathrm{IB}} + c_i - c_i^2 - k.$$

The three cases follow directly from Proposition 2, using the post-switch effort g_i^{IB}. Boundary viability for j is $k \geq g_j^{\mathrm{IB}}$. □

C Comparison with a state-independent ratio-form contest

This appendix replaces the exponential success function by

$$p_i(g_i, g_j) = \frac{g_i}{g_i + g_j}, \qquad p_j = 1 - p_i, \tag{C.1}$$

while retaining the objective (2.1), the fatigue law, $r = 1$, and the regime wedges in (2.10).

C.1 Stationary solution

Player i's Hamiltonian is

$$\mathcal{H}_i = \pi \frac{g_i}{g_i + g_j} - g_i - \rho_i c_i^2 + \lambda_i (g_i + c_i - c_i^2 - k). \tag{C.2}$$

The effort condition is

$$\pi \frac{g_j}{(g_i + g_j)^2} = 1 - \lambda_i = a_i^R. \tag{C.3}$$

The corresponding condition for j is

$$\pi \frac{g_i}{(g_i + g_j)^2} = a_j^R. \tag{C.4}$$

Proposition 14 (Ratio-form stationary regimes)**.** *For any regime profile R,*

$$g_i^R = \frac{\pi a_j^R}{(a_i^R + a_j^R)^2}, \tag{C.5}$$

$$g_j^R = \frac{\pi a_i^R}{(a_i^R + a_j^R)^2}, \tag{C.6}$$

$$p_i^R = \frac{a_j^R}{a_i^R + a_j^R}. \tag{C.7}$$

Thus

$$p_i^{\mathrm{II}} = \frac{1+\rho_j}{2+\rho_i+\rho_j}, \tag{C.8}$$

$$p_i^{\mathrm{BI}} = \frac{1+\rho_j}{2+\rho_j} > \frac{1}{2}, \tag{C.9}$$

$$p_i^{\mathrm{IB}} = \frac{1}{2+\rho_i} < \frac{1}{2}, \tag{C.10}$$

$$p_i^{\mathrm{BB}} = \frac{1}{2}. \tag{C.11}$$

Proof. Adding (C.3) and (C.4) yields

$$\frac{\pi}{g_i+g_j} = a_i^R + a_j^R,$$

so

$$g_i + g_j = \frac{\pi}{a_i^R + a_j^R}.$$

Substitution into the individual first-order conditions gives (C.5) and (C.6). Dividing g_i by total effort gives (C.7). □

The fatigue roots and phase portrait are exactly those in Proposition 2, with g_i^R given by (C.5). The ratio technology differs from the exponential technology because player i's effort depends directly on player j's regime wedge.

For the interior–interior profile,

$$g_i^{\mathrm{II}} = \frac{\pi(1+\rho_j)}{(2+\rho_i+\rho_j)^2}, \tag{C.12}$$

$$g_j^{\mathrm{II}} = \frac{\pi(1+\rho_i)}{(2+\rho_i+\rho_j)^2}. \tag{C.13}$$

If $\rho_i > \rho_j$, then $g_i^{\mathrm{II}} < g_j^{\mathrm{II}}$, so

$$c_i^-(g_i^{\mathrm{II}}) > c_j^-(g_j^{\mathrm{II}}).$$

The weaker player again has the larger recovery region.

C.2 Dynamic reversal under the ratio technology

Proposition 15 (Ratio-form dynamic reversal)**.** *Suppose $\rho_i < \rho_j$. In the interior–interior regime,*

$$p_i^{\mathrm{II}} > \frac{1}{2}.$$

If player j reaches the boundary while player i remains interior, then

$$p_i^{\mathrm{IB}} = \frac{1}{2+\rho_i} < \frac{1}{2}.$$

The boundary player also obtains a strictly larger stationary flow payoff:

$$\begin{aligned} W_j^{\mathrm{IB}} - W_i^{\mathrm{IB}} &= \frac{\pi\rho_i(1+\rho_i)}{(2+\rho_i)^2} + \rho_i\big(c_i^+(g_i^{\mathrm{IB}})\big)^2 \\ &> 0. \end{aligned} \tag{C.14}$$

Proof. The probability statements follow from (C.8) and (C.10). In regime (I,B),

$$g_i^{\mathrm{IB}} = \frac{\pi}{(2+\rho_i)^2}, \qquad g_j^{\mathrm{IB}} = \frac{\pi(1+\rho_i)}{(2+\rho_i)^2}.$$

Therefore

$$\begin{aligned} W_j^{\mathrm{IB}} - W_i^{\mathrm{IB}} &= \pi\left[\frac{1+\rho_i}{2+\rho_i} - \frac{1}{2+\rho_i}\right] - \big(g_j^{\mathrm{IB}} - g_i^{\mathrm{IB}}\big) + \rho_i(c_i^+)^2 \\ &= \frac{\pi\rho_i}{2+\rho_i} - \frac{\pi\rho_i}{(2+\rho_i)^2} + \rho_i(c_i^+)^2, \end{aligned}$$

which yields (C.14). □

C.3 Comparison of contest technologies

The two state-independent contest technologies share the same fatigue mechanism but differ in strategic coupling.

Under the separable exponential technology,

$$g_i^{\mathrm{I}} = \ln\left[\frac{\pi}{2(1+\rho_i)}\right]$$

depends only on player i's own fatigue vulnerability. The opponent affects i's success probability but not its stationary effort.

Under the ratio technology,

$$g_i^{\mathrm{I}} = \frac{\pi(1+\rho_j)}{(2+\rho_i+\rho_j)^2},$$

so both players' fatigue vulnerabilities affect effort and, consequently, the location of each fatigue threshold.

Despite this difference, the reversal mechanism is robust. In both technologies:

(i) the less fatigue-vulnerable player is stronger when both players are interior;

(ii) the player that reaches the boundary removes its fatigue wedge;

(iii) the boundary player obtains a success probability above one half against an interior opponent;

(iv) the boundary player obtains a strictly larger stationary payoff.

The qualitative result is therefore generated by the fatigue regime rather than by a special feature of one contest success function.

C.4 Numerical robustness under the ratio-form technology

For completeness, Figure 10 illustrates the four stationary regime profiles under the ratio-form success function. We set

$$\pi = 3, \qquad \rho_i = 0.10, \qquad \rho_j = 0.35.$$

The exercise is a stationary comparison, so k does not affect the plotted controls or probabilities.

When both players are interior,

$$g_i^{\mathrm{II}} \simeq 0.6747, \qquad g_j^{\mathrm{II}} \simeq 0.5498, \qquad p_i^{\mathrm{II}} \simeq 0.5510.$$

Player i, which is less fatigue-vulnerable, is initially stronger. If player j reaches the boundary while i remains interior, the regime becomes (I, B) and

$$g_i^{\mathrm{IB}} \simeq 0.6803, \qquad g_j^{\mathrm{IB}} \simeq 0.7483, \qquad p_i^{\mathrm{IB}} \simeq 0.4762.$$

Thus the effort ranking and the success ranking reverse, exactly as in the exponential specification.

The comparison also illustrates the principal technological difference. In the ratio contest, a change in one player's fatigue wedge changes both effort choices even without territorial

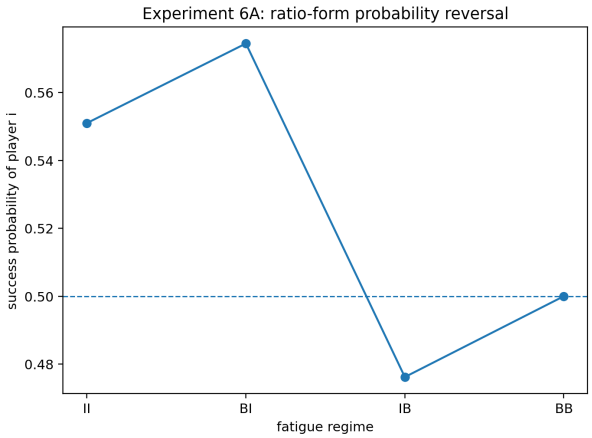

(a) Success probability across regimes.

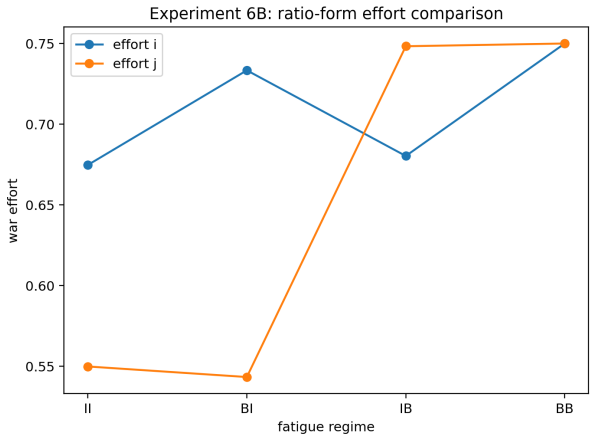

(b) Regime-specific effort choices.

Figure 10: Numerical robustness of the reversal mechanism under the state-independent ratio-form success function.

state dependence. In the state-independent exponential contest, by contrast, separability prevents this cross-player control response. The probability-reversal mechanism is therefore robust, whereas the degree of strategic coupling depends on the contest technology.